CCN SCAVENGING AND DRIZZLE

Stephen Noble
and
James G. Hudson
Desert Research Institute
Reno, Nevada

1. INTRODUCTION

The effect of preexisting or precloud aerosol on cloud microphysics is fundamental to cloud physics. Interest is piqued by the wide range of observed aerosol and cloud droplet concentrations, compositions, and size distributions. The fact that a large but as yet unknown component of the aerosol is of anthropogenic origin gives rise to the indirect aerosol effect(IAE), which is the largest climate uncertainty.

IAE consists of at least two components: 1st IAE the effect on cloud radiative properties—i.e., higher cloud droplet concentrations producing brighter clouds, and 2nd IAE precipitation inhibition due to smaller droplets. Both subjects are addressed here in a study that builds upon Hudson and Mishra [2007] (hereafter HM7). That study was from the RICO project (Rauber et al. 2007), which was done in December-January 2004-05 in the northeastern Caribbean. Measurements presented in HM7 and here were all from the NCAR C-130 airplane. HM7 showed both of the expected effects of aerosol, namely cloud condensation nuclei (CCN) concentration variations, on cloud microphysics. However, the analysis of HM7 was limited to only the early stages of cloud development near the bases of the small cumulus clouds that were studied. Although HM7 did find a strong positive correlation of CCN concentrations with cloud droplet concentrations (N_c) [1st IAE] and a strong negative correlation with mean cloud droplet sizes from the FSSP (2nd IAE), the analysis was restricted to cloud parcels with liquid water content (LWC) greater than 0.25 g m^{-3}, updrafts (w) exceeding 0.5 m/s and altitudes of 600-900m. Although that article demonstrated the greater influence of CCN than giant nuclei (GN) on precipitation initiation, the limits placed on that analysis did not really demonstrate the effects of CCN on either cloud radiative properties or precipitation. For instance it has been suggested that dynamical processes could washout initial aerosol effects at cloud base [e.g., Baker et al. 1979]. Thus at higher altitudes where cloud radiative properties are of greater importance and where precipitation is usually initiated the effect of the subcloud CCN effect may be washed out. Entrainment may have more influence on cloud microphysics at higher altitudes and moreover the CCN concentrations in the entraining air may also be different from the subcloud concentrations. To address these issues this analysis broadens all aspects of HM7—LWC, w, droplet/drop sizes, and altitude.

2. RESULTS

Table 1 shows the consideration of three more flights than HM7, RF4, 11 and 17 (D10, J7 and J19). Figure 1 expands Figure 2a of HM7 by including all parcels with LWC > 0.1g m^{-3}. This adds two data points, two more flights. The CCN-cloud droplet concentration (N_c) correlation coefficient (R) is not diminished by this expansion of cloud parcels and flights, but is actually higher (0.85 versus 0.80) than that of the more restricted analysis of HM7. The slope of the linear regression is diminished from

1.08 to 0.60 because these cloud parcels have lower average concentrations while the low magnitude intercept is nearly identical. Restricting this analysis to only the same 14 flights reported by HM7, results in only a further increase of R to 0.88. When the data is further expanded by considering a lower LWC threshold of 0.01 g m^{-3}, R increases to 0.88 for the 16 flights and 0.89 for the 14 flights considered by HM7. This expansion actually allows the inclusion of RF17, so that this R for 17 flights is 0.89. Further expansion of the data under consideration by using an even lower LWC threshold of 0.001 g m^{-3}, results in a further increase of R to 0.90 for 16 flights, 0.91 for 14 flights and 0.92 for 17 flights.

Figure 2 shows that droplet concentrations were roughly similar with altitude. Figures 3 and 4 show that the CCN-N_c correlations diminished only slightly with altitude even as the average N_c concentrations decreased with altitude (smaller regression slopes). Rather than the gross measure of the overall droplet spectra expressed by the mean of the FSSP distribution we now examine CCN correlations with droplet concentrations that exceed various threshold sizes. Figure 5 shows how R reverses for larger droplets. Figures 6 and 7 show how R changes with altitude for the various droplet size thresholds. Figure 6 considers all of the flights that had data at the various altitude bands, but this means different numbers of flights at the different altitudes. The different flights among the different altitudes may bias the data, so Figure 7 considers data from only the same eight flights that had data at the same five altitude bands. The smallest droplet size thresholds have rather similar large positive R values at all levels, whereas the largest cloud droplets have negative R at all levels and similar large negative R at all but the lowest levels. Intermediate droplet size thresholds shift from low positive or high negative values at low altitudes to high positive values at higher altitudes as a result of greater droplet sizes at higher altitudes. This results in greater droplet concentrations for the higher threshold sizes. The lower R for the small droplets (total droplets N_c) in the 1500-1800m altitude band in Fig. 6 is due to the RF9 data. RF9 small droplet concentrations are a significant outlier in this altitude range as they are more than 100 cm^{-3}, whereas N_c is for RF9 is less than 50 cm^{-3} at the lower altitudes. This was probably due to the fact that an especially large CCN concentration “spike” was measured during the 100m altitude circles on RF9. As noted by HM7 these usually small concentration spikes that occurred during most flights were removed from calculation of the averages. Apparently that high CCN concentration air parcel measured on RF9 produced some cloud parcels with high droplet concentrations and those parcels happened to be observed only in this altitude range. This anomalously low R is not displayed in Fig. 7 because RF9 was not one of the eight flights displayed in this figure because it did not have data at all altitudes.

Figure 8 shows the increase in the concentration of large cloud droplets at higher altitudes as the droplets grow in size because of the lower temperatures at the higher altitudes; more water is condensed on the same droplets as the same parcels of air move upward. Figures 9 and 10 display the negative correlations of these large droplet concentrations with the surface CCN concentrations. In these figures the data seems to split along two separate regression lines that have much greater negative R noted in the caption. This split of the flights may be indicative of other influences on cloud microphysics such as dynamics that may have common manifestations for these two sets of flights. Figure 11 shows that the negative R continues to higher altitudes and further out in the tail of the droplet distribution. Figure 12 shows that a higher order regression produces a much higher R suggesting that the effect of CCN on the tail of the droplet distribution may be nonlinear.

Figures 13-16 show the vertical distributions of drizzle drop concentrations measured with the 260X probe. The large differences in drizzle drop concentrations require a log scale. This shows the increase in drizzle with altitude. Figures 17 and 18 show that there is no correlation of drizzle concentrations with CCN concentrations in the lowest cloud layers. On the other hand Figures 19 and 20 show that there is a negative correlation of surface CCN with drizzle at a higher altitude range. These figures show divisions of the flights along the same lines as in Figs. 9 and 10 for cloud droplets. This again may indicate groupings of data from certain flights because of other factors such as dynamics that are common to each group of flights. Figures 21-24 show how the correlations of CCN with drizzle go with altitude. Figures 21 and 22 display all of the data whereas Figures 23 and 24 are restricted to the same eight flights for all levels displayed. All correlations are negative albeit very week for the cloud base layer. R generally increases in magnitude with altitude. R is generally lower in magnitude for the larger drizzle drops except at cloud base. Figure 25 displays the same data shown in Figs. 6, 21 and 22 with R plotted against threshold diameter for each altitude range. Likewise Figure 26 shows the same data as in Figs. 7, 23 and 24.

Figure 27 is like Figs. 25 and 26 except that it shows R as function of threshold cloud droplet diameter for various LWC bins only in the 600-900m altitude range. Similar high positive R is seen for all LWC up to 10 µm threshold droplet diameter. Between 10 and 20 µm diameter R plunges to extreme negative values of 0.7-0.8 and then gradually decreases in magnitude for larger droplets. The only positive R above 20 µm is for the 40 µm droplets in the lowest LWC bin. Figure 28 displays the same data as a function of LWC bins for each cumulative diameter. The similarity of R for most LWC bins is significant. The only exception is the one just mentioned and 15 µm, which transitions from the tail of the distributions in the low LWC bins (negative R) to a greater share of the cloud droplets in higher LWC bins (positive R).

Figures 29 and 30 show the same data as Figs. 27 and 28 for the next higher altitude range (900-1200m). Since there is more condensed water at higher altitudes there are more LWC bins. The positive R for total cloud droplets (N_c) are even greater in magnitude (~0.9) for all but the two extreme LWC bins. Because of the greater droplet sizes, R continues to be uniformly high out to 15 µm. The plunge to negative R then occurs between 15 and 25 µm, again larger than at the 600-900m altitude because the droplets are larger. The size where the plunge takes place is generally higher for higher LWC. The maximum magnitude of the negative R here is 25 rather than 20 µm and it is greater in magnitude than the 600-900m range (0.8-0.9 compared to 0.7-0.8). The gradual decrease in magnitude of R is much less than the 600-900m range and is never anywhere near positive. The least negative R above 25 µm is for the lowest LWC bin. In spite of the low positive R for the two extreme LWC bins for total droplets the negative R for diameter 25 µm is similar to the other LWC bins. The highest LWC bin shows the most negative R above 30 µm. The more extreme R values of this higher altitude range are apparent by comparing Fig. 30 with Fig. 28. Here the transition size is 20 rather than 15 µm. Figure 31 continues to higher LWC but these LWC are observed only for a more limited number of flights as noted in the caption. On the other hand a larger number of flights are available here for the lower LWC bins.

Figures 32-34 are comparable to Figs. 29-31 for the next higher altitude range (1200-1500m). These show mostly the same overall trend of positive R for small sizes and negative R for large sizes. However, the R values are of much lower magnitude indicating that the CCN have less influence at this higher altitude that is further from the CCN measurements. Notable is the negative or lack of correlation for the lowest two LWC bins at the small sizes. However R is positive at least for the 15 and 20 µm sizes for these LWC bins.

Figures 35-37 are comparable to Figs. 32 and 33 for the next higher altitude range (1500-1800m). Here the correlations are of slightly greater magnitude than they were for 1200-1500m but not nearly as great as for the lowest two altitude ranges.

3. CONCLUSIONS

The results presented here show that CCN concentrations exert ubiquitous effects on cloud microphysics. Strong correlations were found not only between CCN concentrations and total cloud droplet concentrations but just as strong negative correlations were found between CCN and large cloud droplets and drizzle droplet concentrations. These strong correlations continued from cloud base for more than 2 km in altitude. The correlations extended to nearly all liquid water content levels in these small cumulus clouds. This study confirms and extends HM7 that CCN are the aerosol that exerts the most influence on cloud microphysics—both on cloud radiation and precipitation properties. Moreover, this was observed in air masses that all were within the traditional maritime regime; i.e., concentrations less than 200 cm^{-3}. These results uphold the basis for both the 1st and 2nd indirect aerosol effects (IAE).

Acknowledgements.

This work was supported by US NSF grant ATM-0342618.

References

Baker, M.B., R.G. Corbin, and J. Latham, 1979: The evolution of droplet spectra and rate of production of embryonic raindrops in small cumulus clouds. *J. Atmos. Sci*., **36**, 1612-1615.

Hudson, J. G., and S. Mishra (2007), Relationships between CCN and cloud microphysics variations in clean maritime air, *Geophys. Res. Lett*., **34**, L16804, doi:10.1029/2007GL030044.

Rauber, R.M., et al., 2007: Rain In shallow Cumulus over the Ocean, the RICO campaign. *Bulletin, AMS*, 88, 1912-1928.

flight	date	N_c HM7	N_c LWC>0 .1gm^{-3}	N_c HM7	N_c LWC> 0.1gm^{-3} rank	CCN	CCN rank	Dur LWC> 0.1	Dur LWC >0.01	Dur LWC> 0.001
RF01	D07	201	108	2	1	200	1	601	1011	1293
RF02	D08	123	77	4	3	133	3	30	113	173
RF03	D09	74	39	12	11	98	9	230	629	868
RF04	D10	--	32	--	--	92	11	22	357	663
RF05	D13	71	30	13	13	91	12	92	212	331
RF06	D16	111	64	7	4	131	4	270	924	1308
RF07	D17	46	25	14	14	55	16	73	379	620
RF08	D19	98	48	9	10	79	15	266	875	1299
RF09	D20	74	38	11	12	94	10	128	335	414
RF10	J05	80	52	10	9	108	8	224	666	900
RF11	J07	--	62	--	--	86	14	60	383	601
RF12	J11	135	63	3	5	90	13	181	482	608
RF13	J12	114	61	5	6	119	6	226	842	1375
RF14	J14	207	102	1	2	142	2	211	754	1145
RF15	J16	112	57	6	7	108	7	141	362	528
RF17	J19	--	--	--	--	48	17	--	1	5
RF18	J23	104	55	8	8	126	5	142	331	411
ave		111				106				
sd		46				35				

Table 1. Flight number; date; flight-averaged concentrations of cloud droplets (N_c) (cm^{-3}) from Table 1 HM7 (LWC > 0.25 gm^{-3}; updraft > 0.5 m/s, 600-900m altitude), N_c for LWC > 0.1gm^{-3}, 600-900m altitude; rank order of N_c (HM7) (not the rank shown in in HM7 but the rank of all 14 flights considered by HM7; rank order of N_c(0.1gm^{-3}) CCN concentrations at 1% S (cm^{-3}) at 100m altitude (same as HM7 but 3 extra flights); and rank order of CCN concentrations. Duration (number of seconds) of data in each LWC category. Everything in this table pertains to 600-900m altitude.

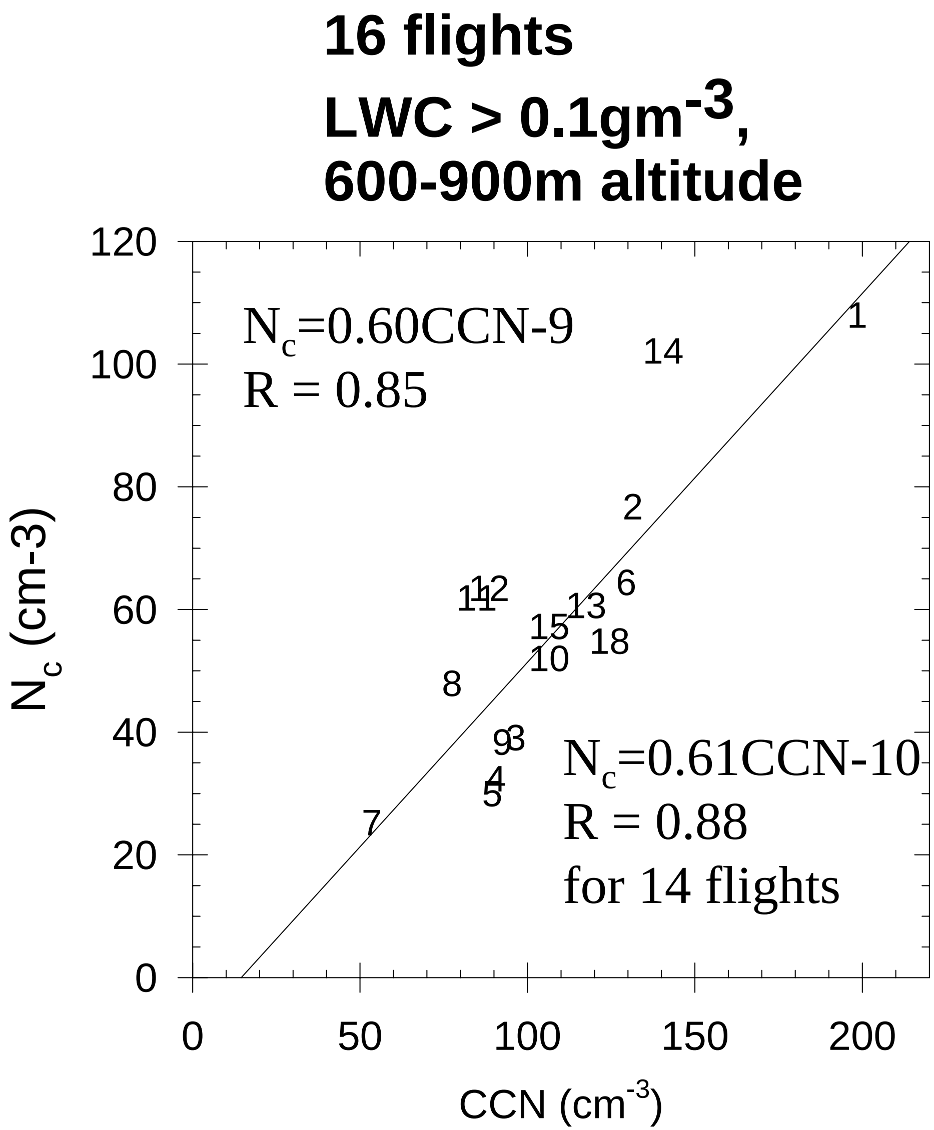

Figure 1. Average total (>2.4 µm) FSSPdroplet concentrations (N_c) measured during each flight within the denoted altitude and LWC range against the average 100m altitude CCN concentrations at 1% S for each flight. Data points are plotted as the flight number (Table 1). All of the 17 flights under consideration here with the exception of RF17 (J19) had clouds within this altitude range. The linear regression line, equation and correlation coefficient (R) are shown as well as the linear regression and R for only the same 14 flights considered by HM7. This excludes RF4 and 11 (D10 and J7).

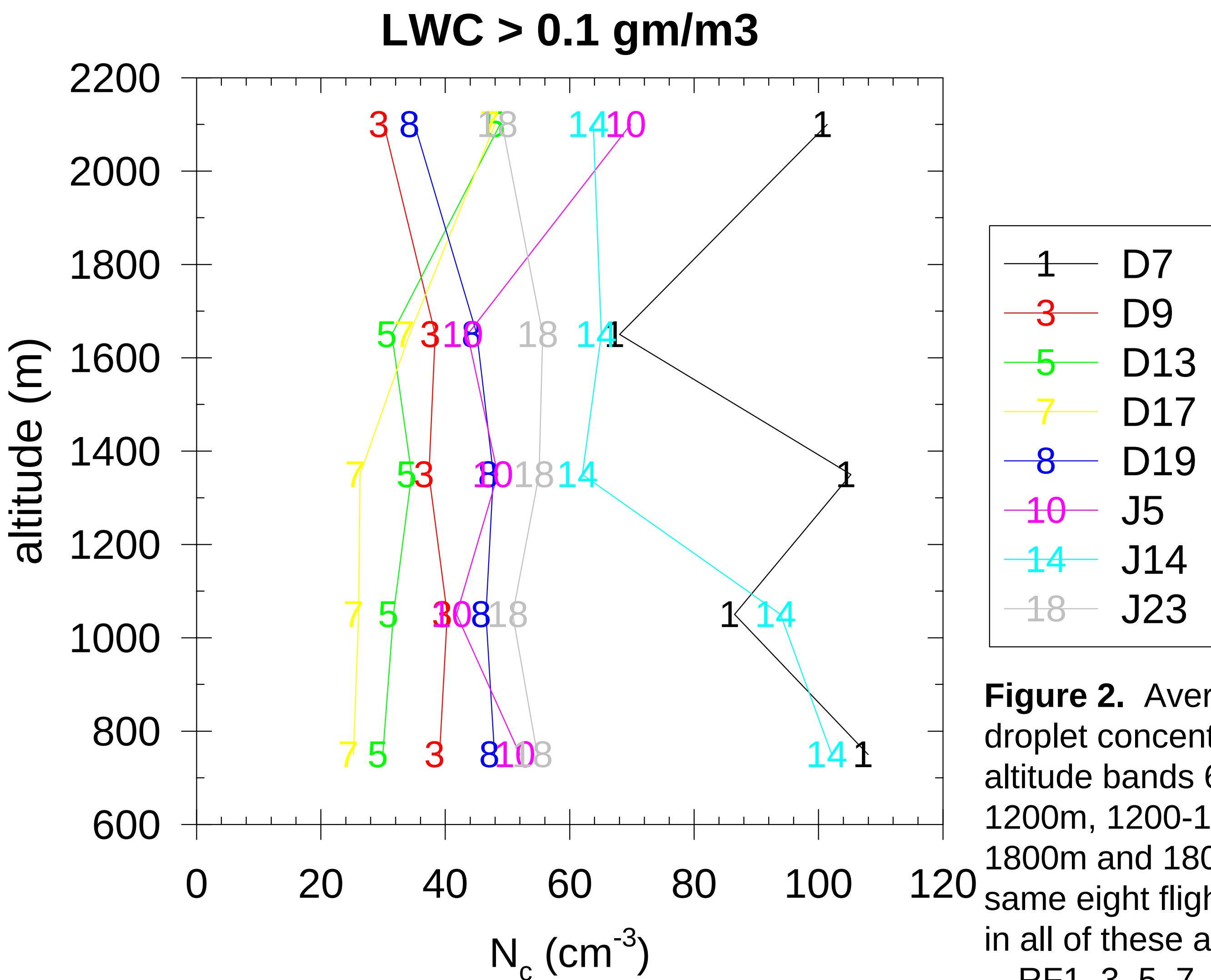

Figure 2. Average total cloud droplet concentrations within altitude bands 600-900m, 900-1200m, 1200-1500m, 1500-1800m and 1800-2400m for the same eight flights with clouds in all of these altitude ranges —RF1, 3, 5, 7, 8, 10, 14 and 18 (D7, D9, D13, D17, D19, J5, J14 and J23).

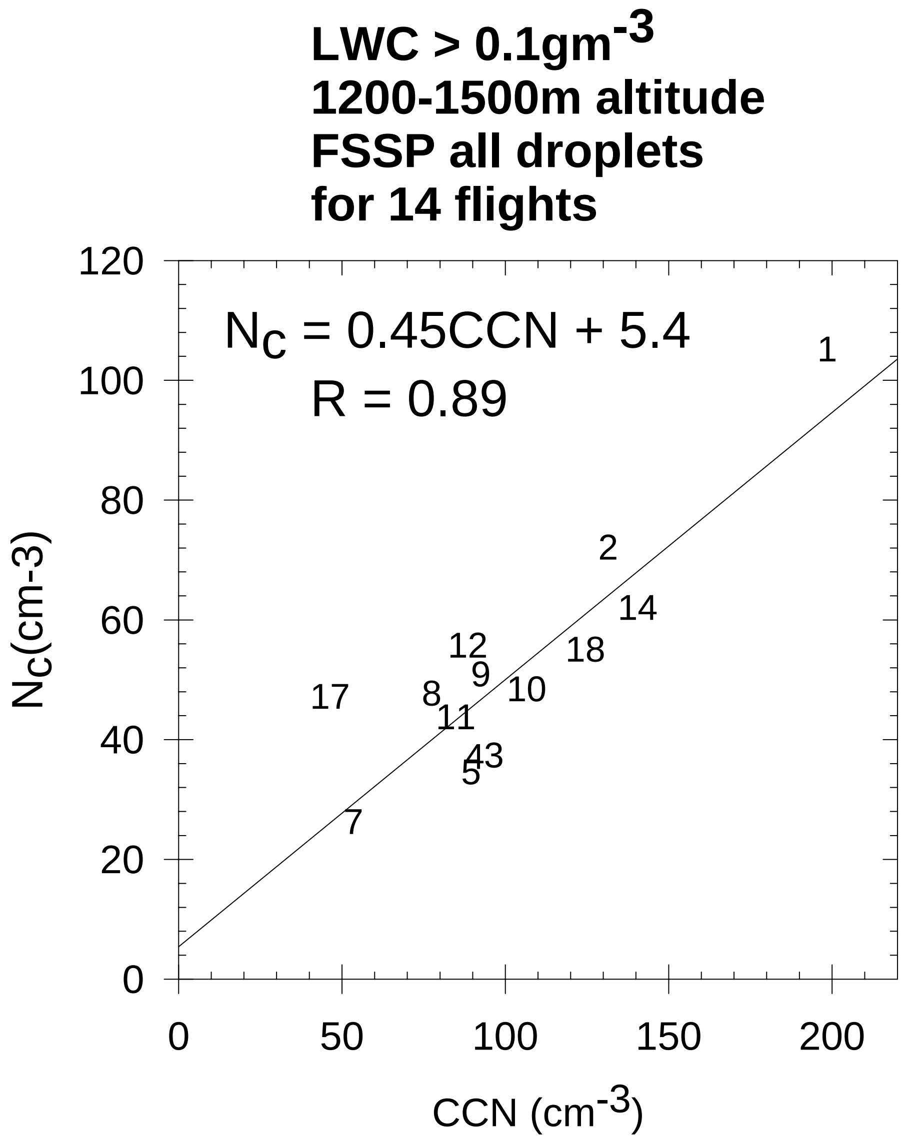

Figure 3. As Fig. 1 but for a higher altitude range and a different missing flight, RF6 (D16) that did not have cloud data in this altitude range. Note the lower N_c range.

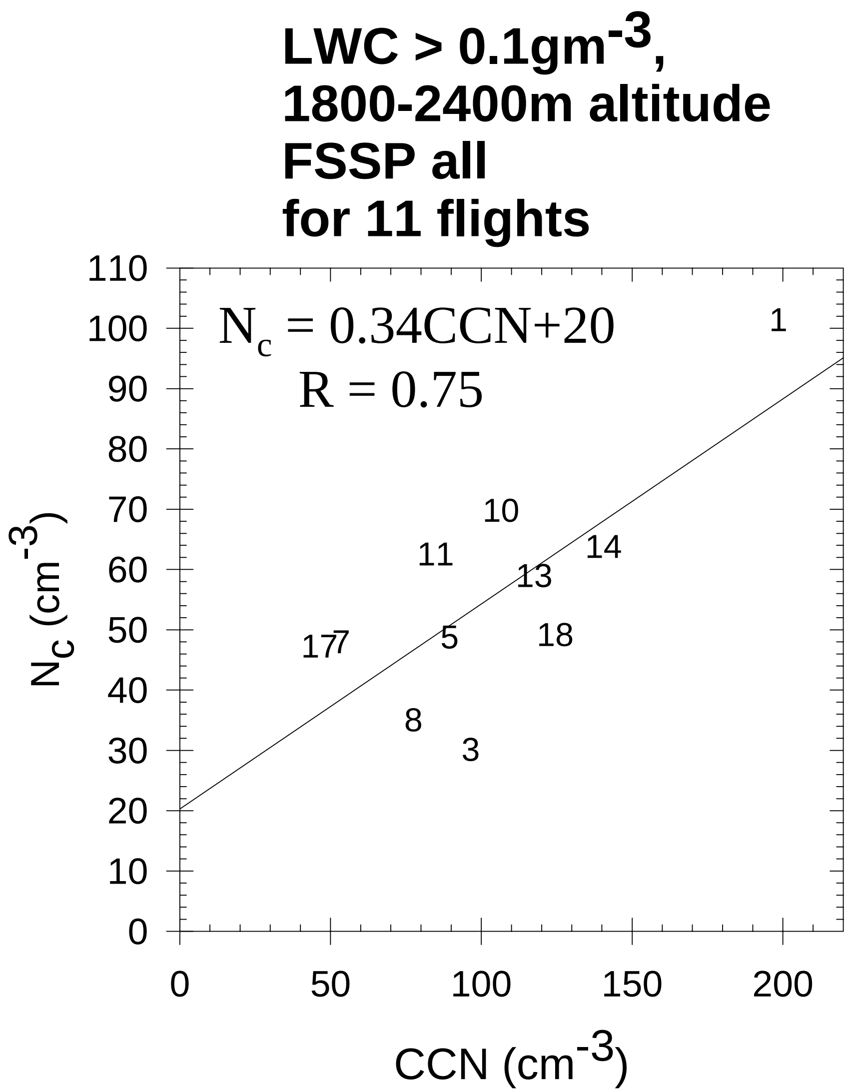

Figure 4. As Fig. 3 but for an even higher altitude range that had fewer flights with cloud data in this altitude range; no data from RF2, 4, 6, 9, 12 or 15 (D8, D10, D16, D20, J11 and J16).

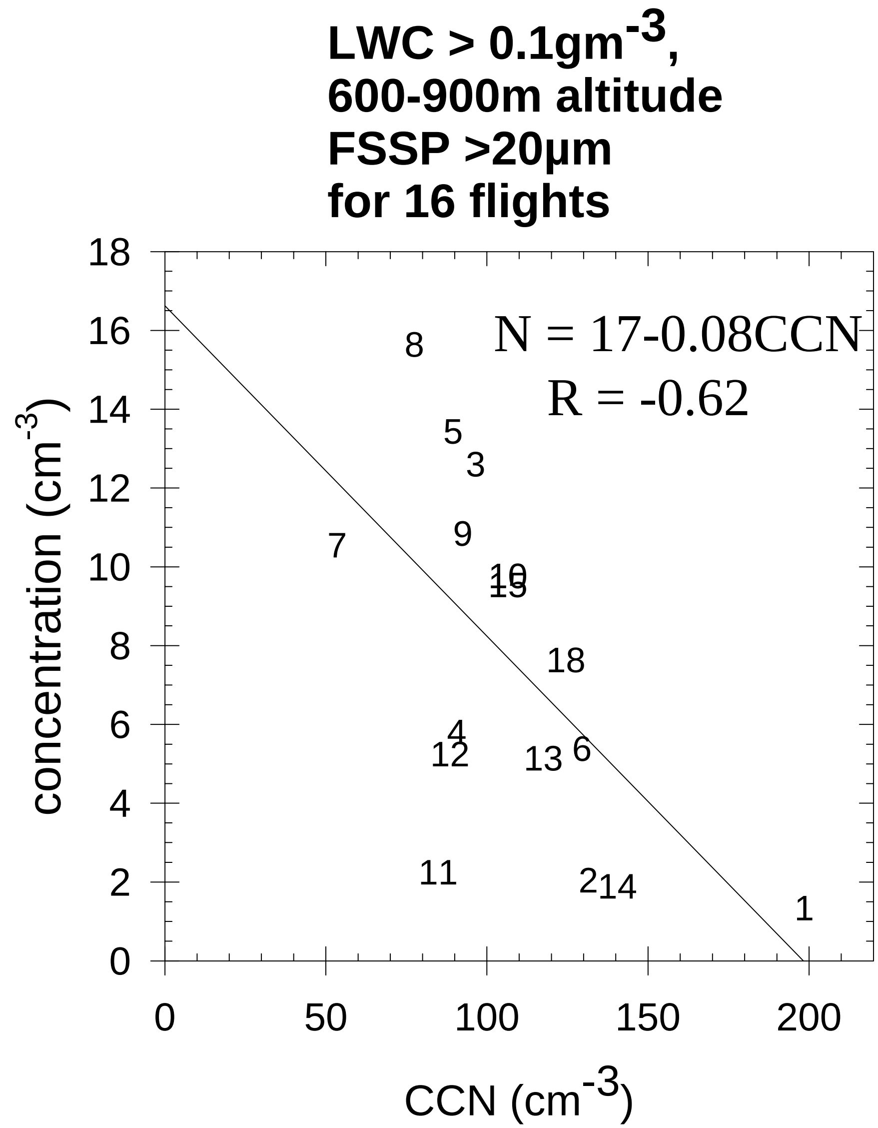

Figure 5. As Fig. 1 but only for larger cloud droplets. Note the much smaller droplet concentration range.

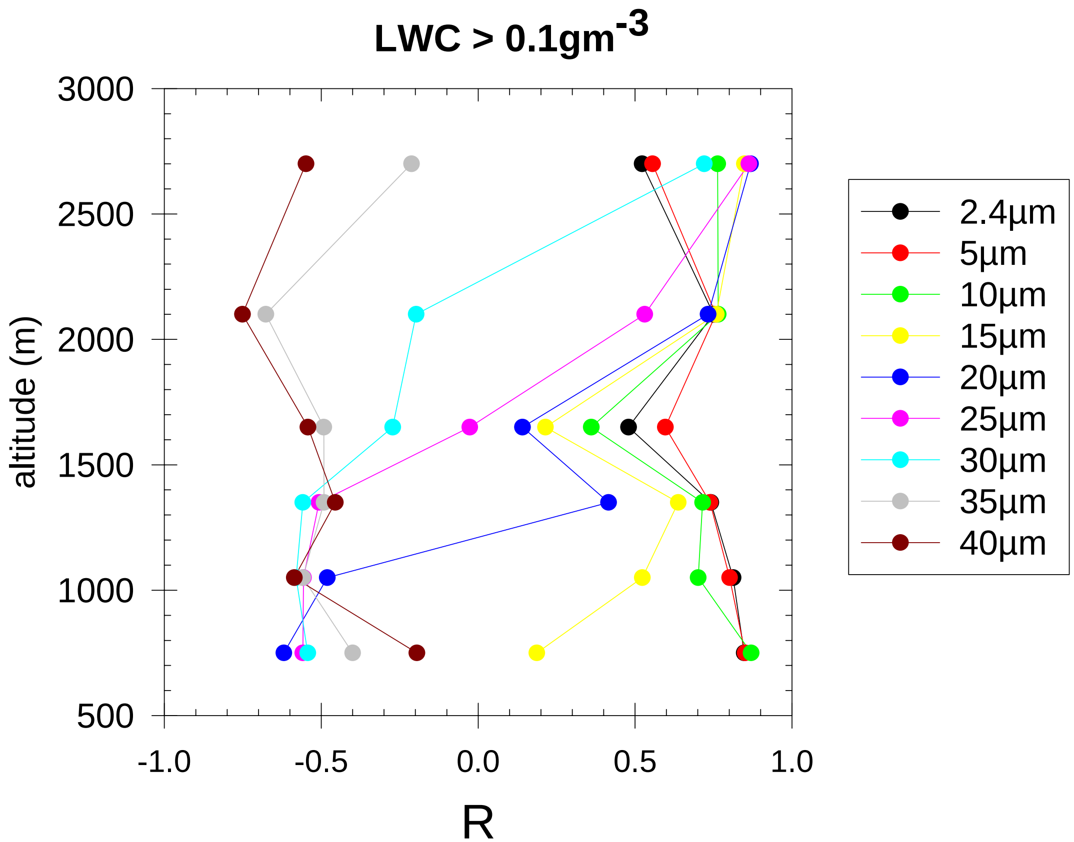

Figure 6. Correlation coefficients (R) as a function of altitude for CCN at 1% S measured during the half hour circles at 100m altitude versus cumulative cloud droplet concentrations measured within various altitude bands. Cloud is defined here as LWC > 0.1 gm-3. The number of flights and the actual flights considered at each altitude here were different because there were not always clouds within some of the altitude bands for some of the flights. 600-900m—16 flights (no RF17); 900-1200m—15 flights (no RF13 or 17); 1200-1500m—16 flights (no RF6); 1500-1800m—13 flights (no RF2, 4, 6 or 11); 1800-2400m—11 flights (no RF2, 4, 6, 9, 12 or 15); 2400-3000m—6 flights (no RF2, 4, 5, 6, 8, 9, 10, 12, 14, 17 or 18).

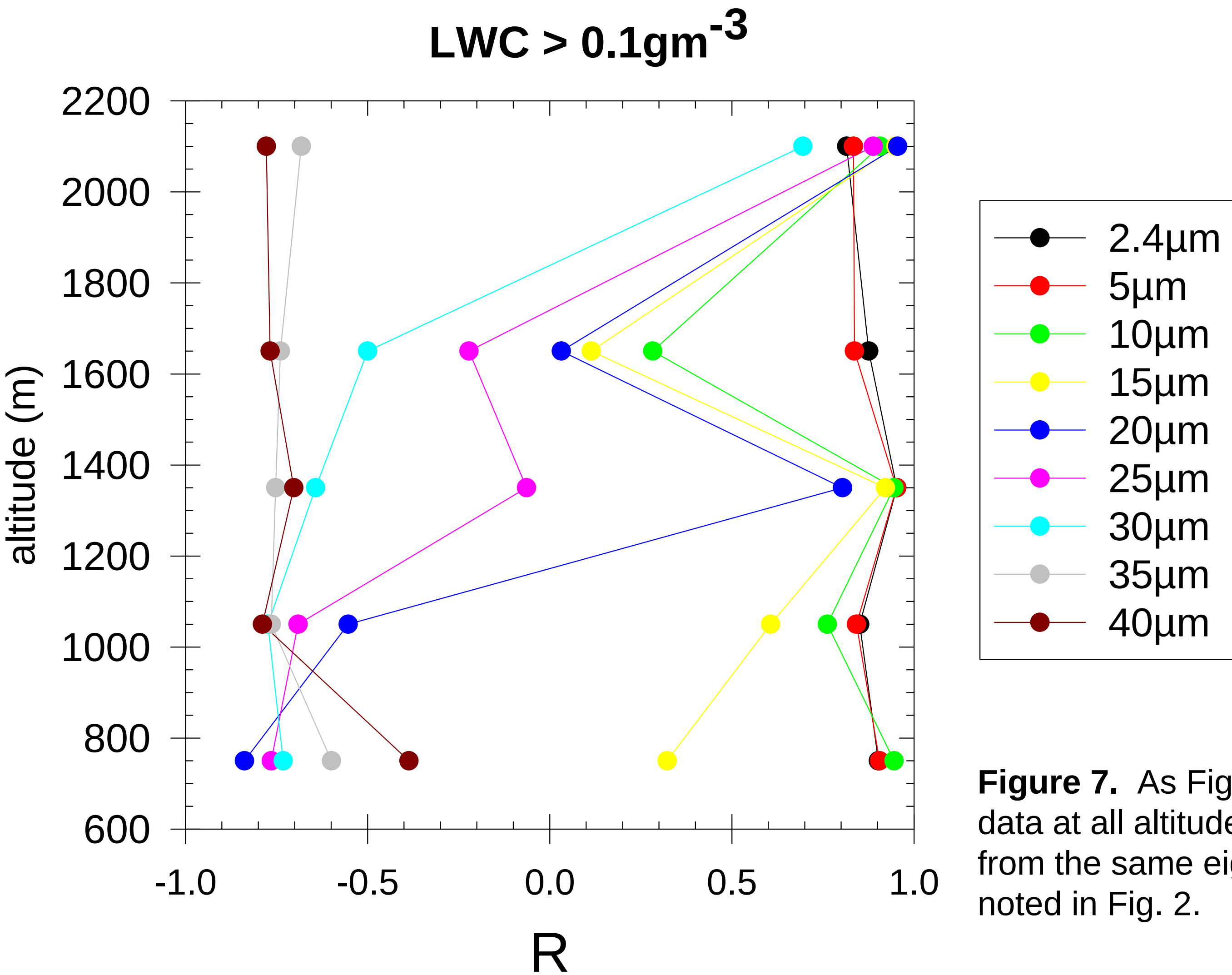

Figure 7. As Fig. 6 but all data at all altitudes are from the same eight flights noted in Fig. 2.

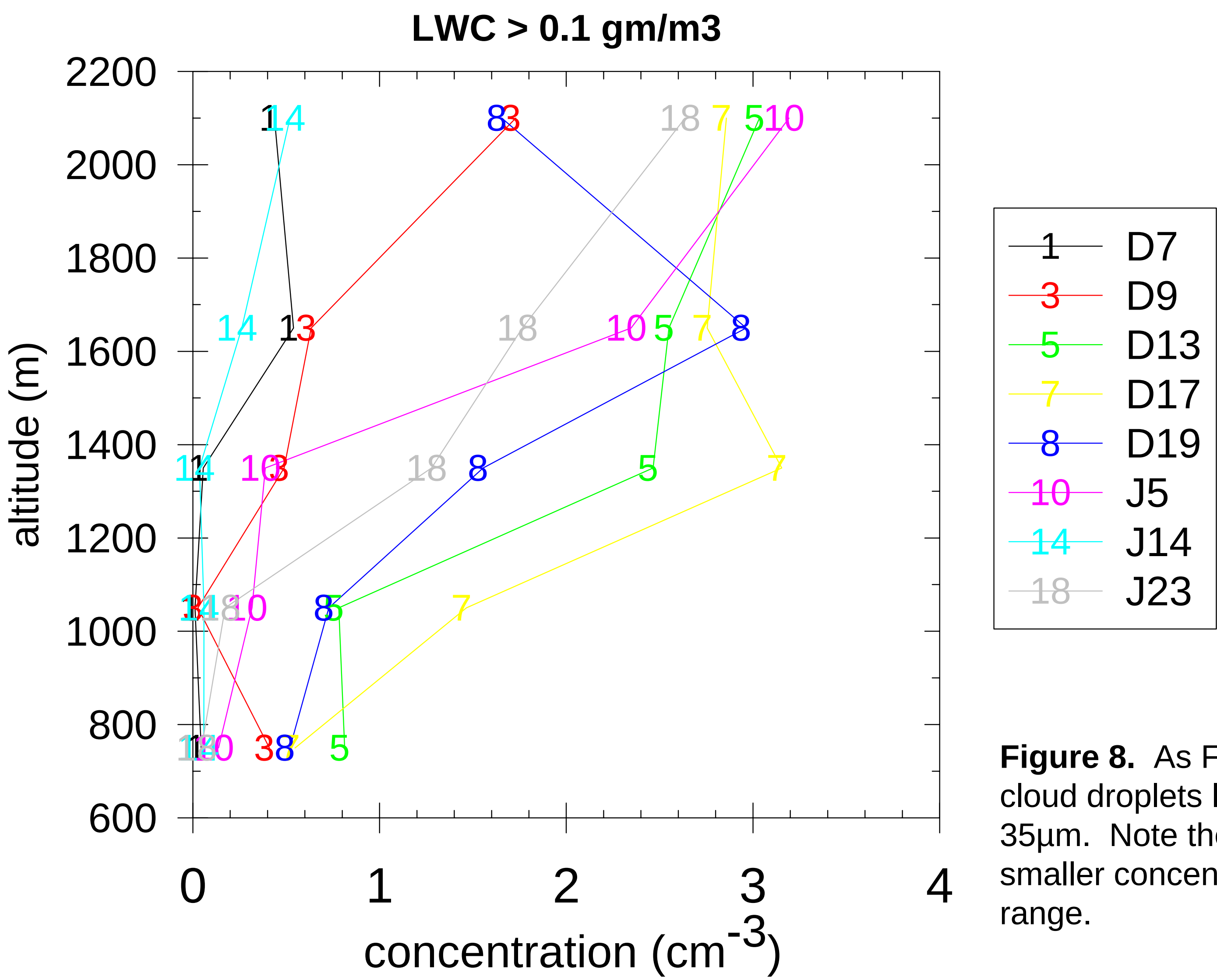

Figure 8. As Fig. 2 but for cloud droplets larger than 35µm. Note the much smaller concentration range.

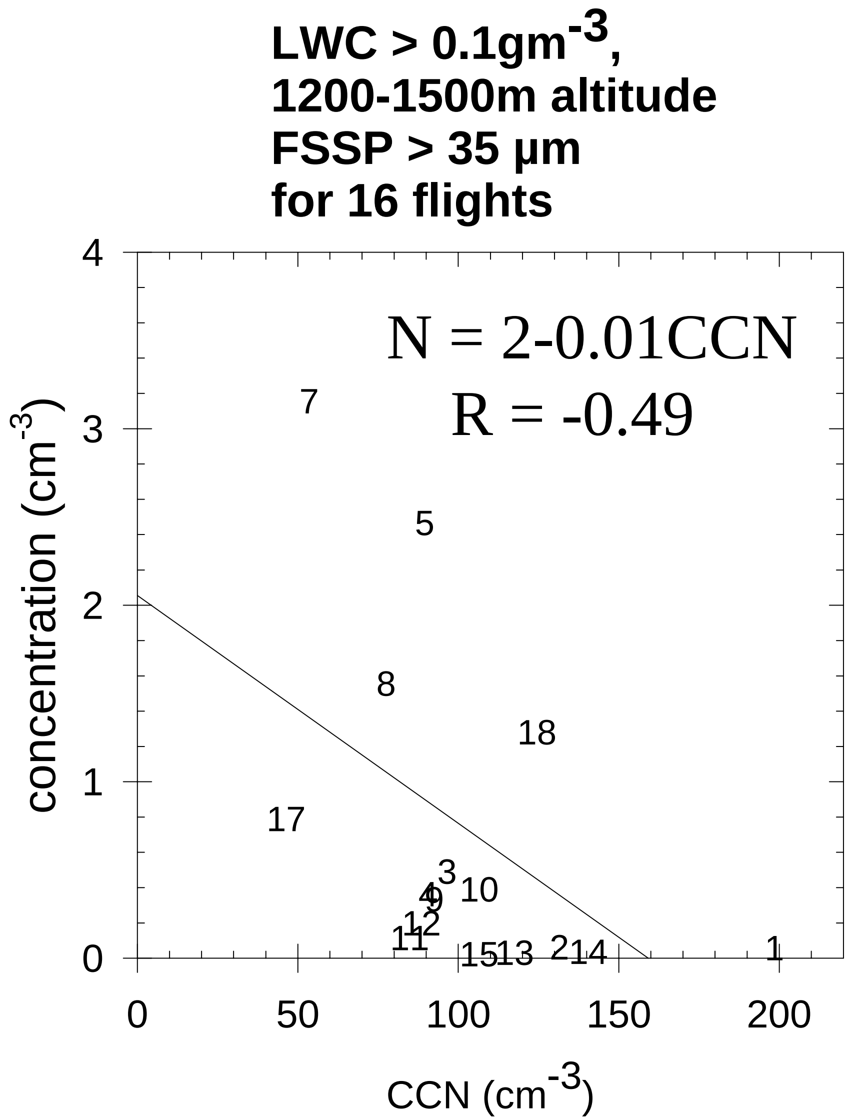

Figure 9. As Fig 5 but for an even larger size range and a higher altitude. Note the smaller droplet concentration range. If only RF1, 5, 8, 7 and 18 are considered R is -0.92. R for the other 11 flights displayed here is -0.77.

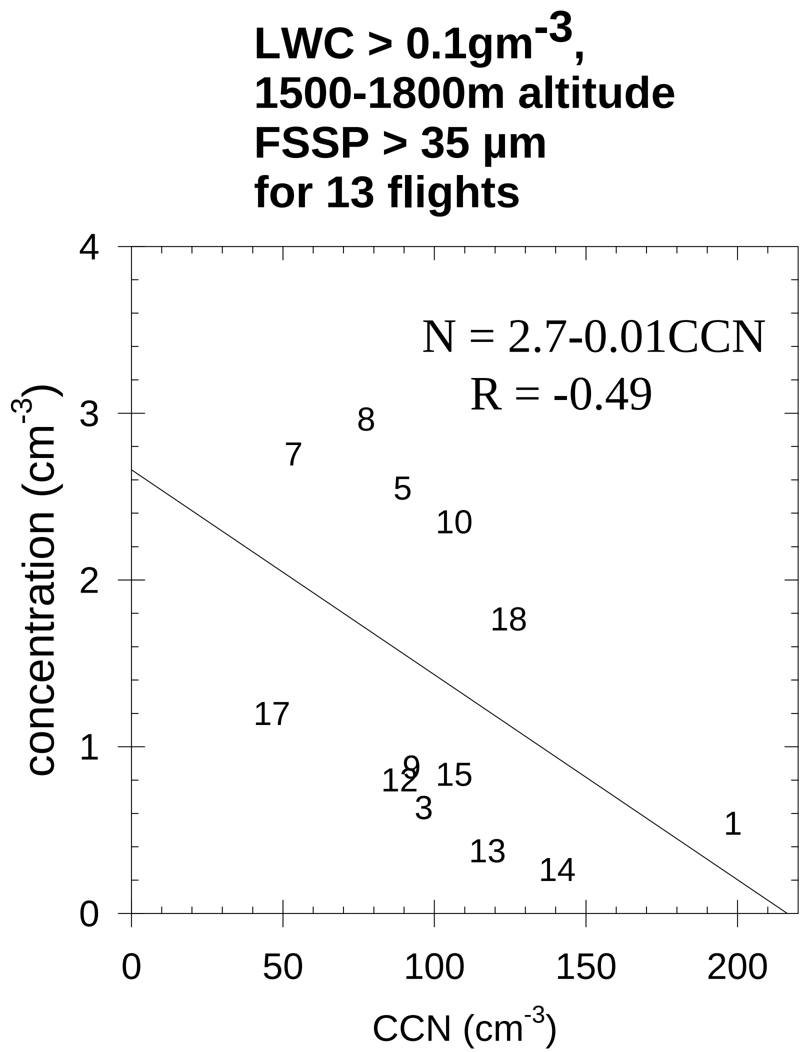

Figure 10. As Fig. 9 but for the next altitude range, which has 3 fewer flights (see Fig. 6 caption). If only RF1, 5, 7, 8, 10 and 18 are considered R is -0.97. This is the same group first separately considered in Fig. 9 except for the addition of RF10. R for the other seven flights in this figure is -0.93.

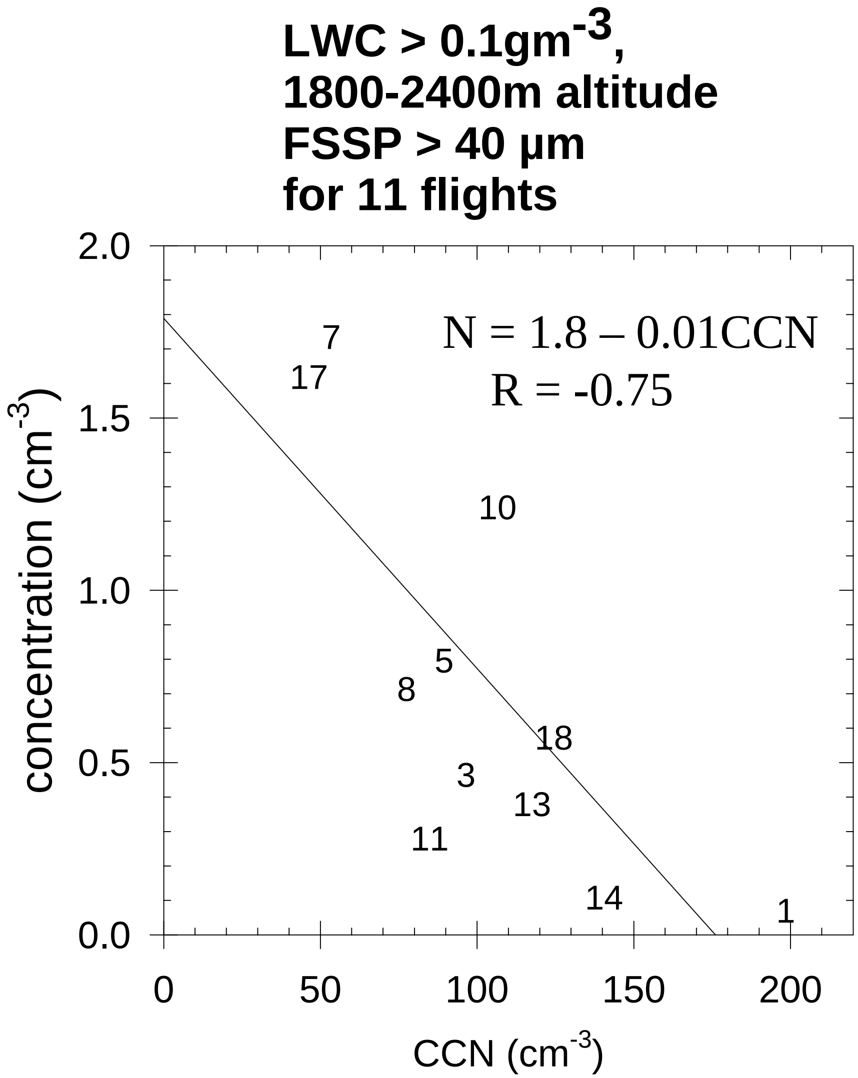

Figure 11. As Fig. 10 but for the next higher altitude range, which has two fewer flights (see Fig. 6 caption) and the next larger droplet size range. Note the even smaller droplet concentration range.

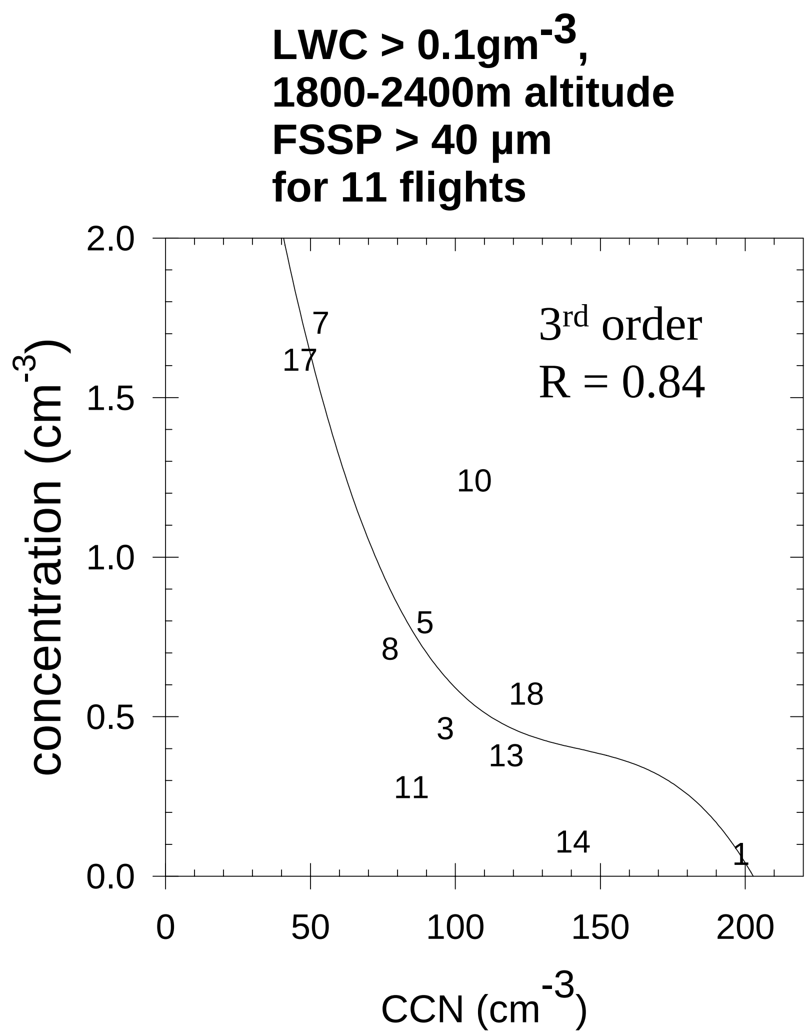

Figure 12. As Fig. 11 but for 2nd order regression.

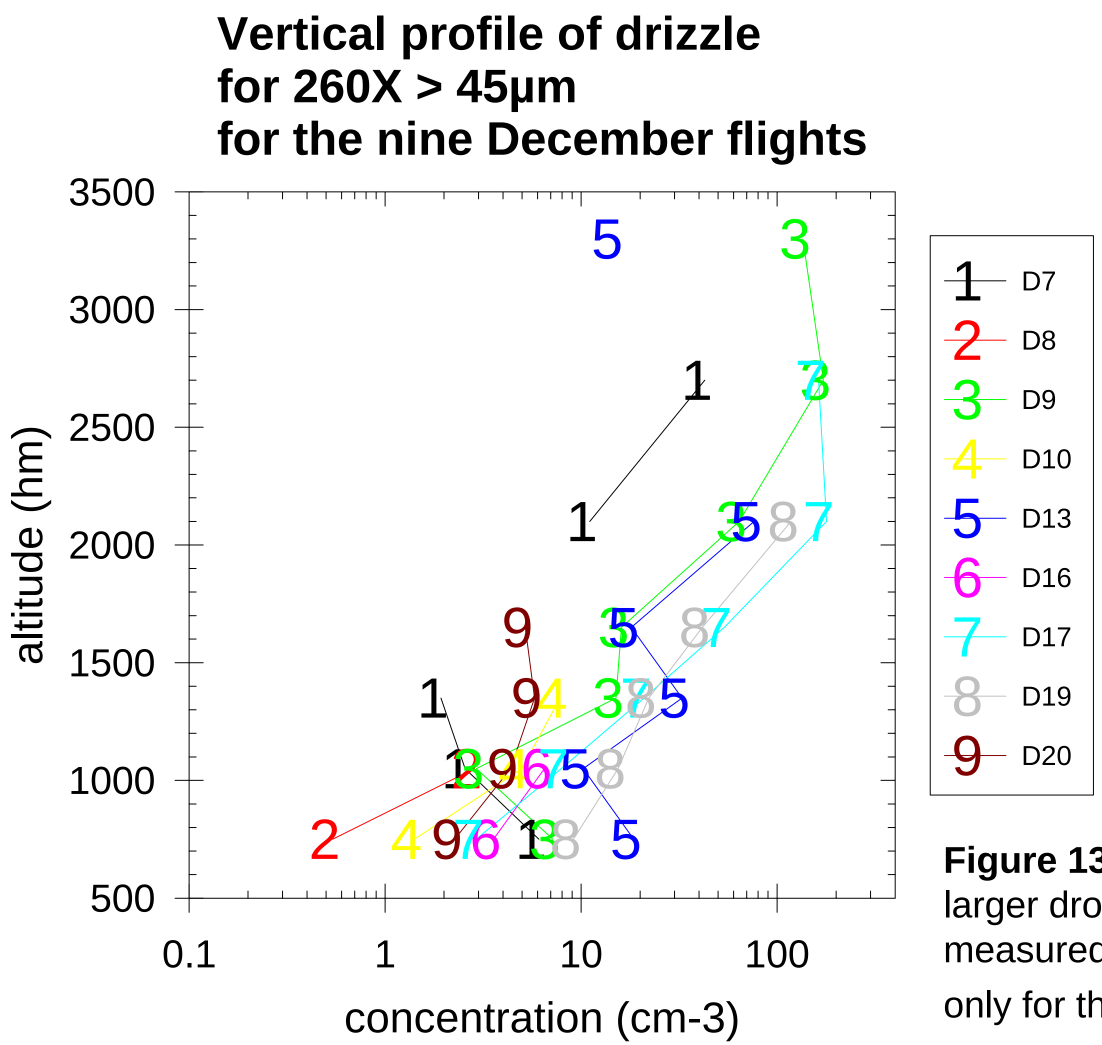

Figure 13. As Fig. 8 but for even larger drops (> 45 µm; drizzle) measured with the 260X probe only for the December RICO flights.

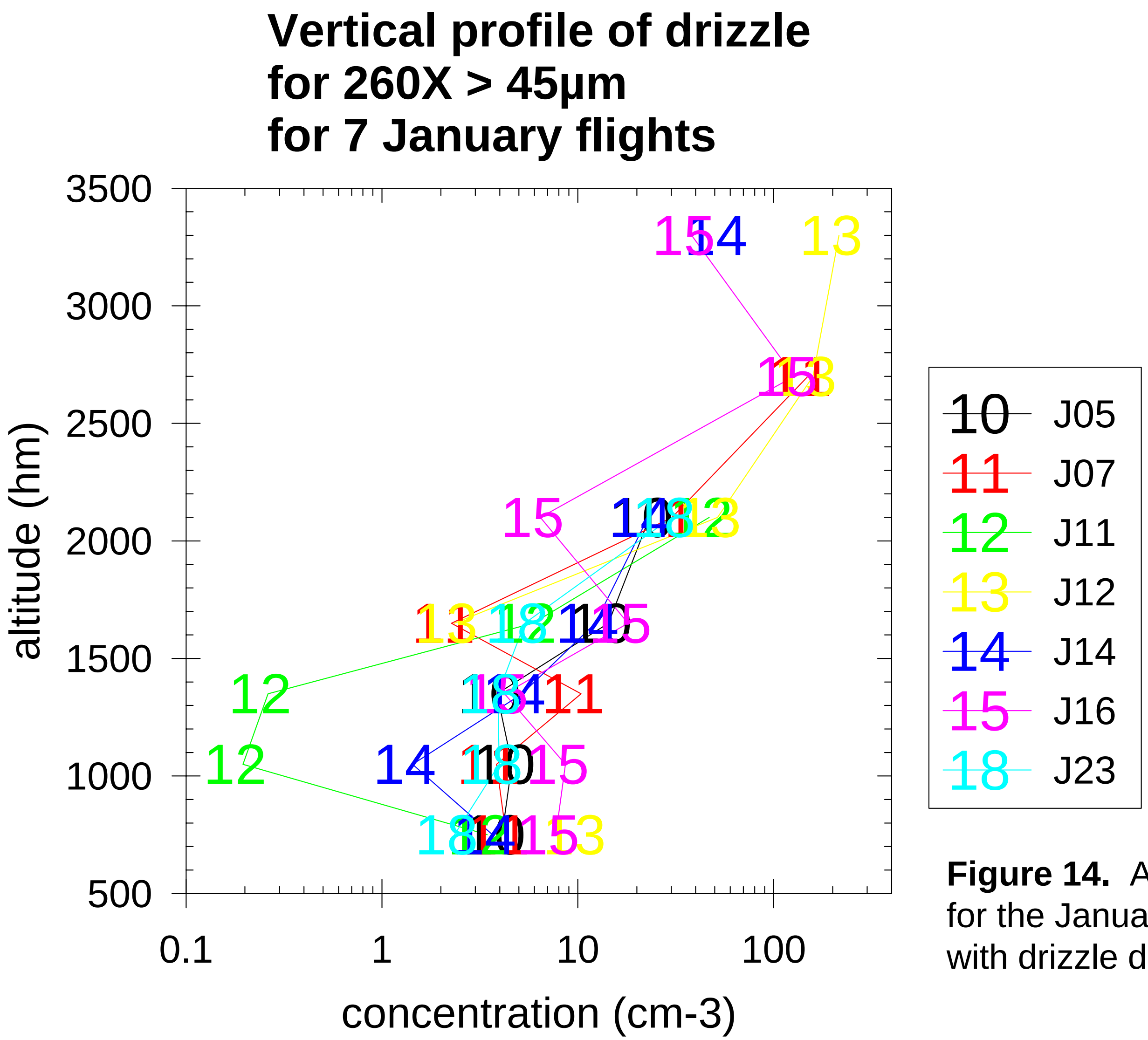

Figure 14. As Fig. 13 but for the January RICO flights with drizzle data.

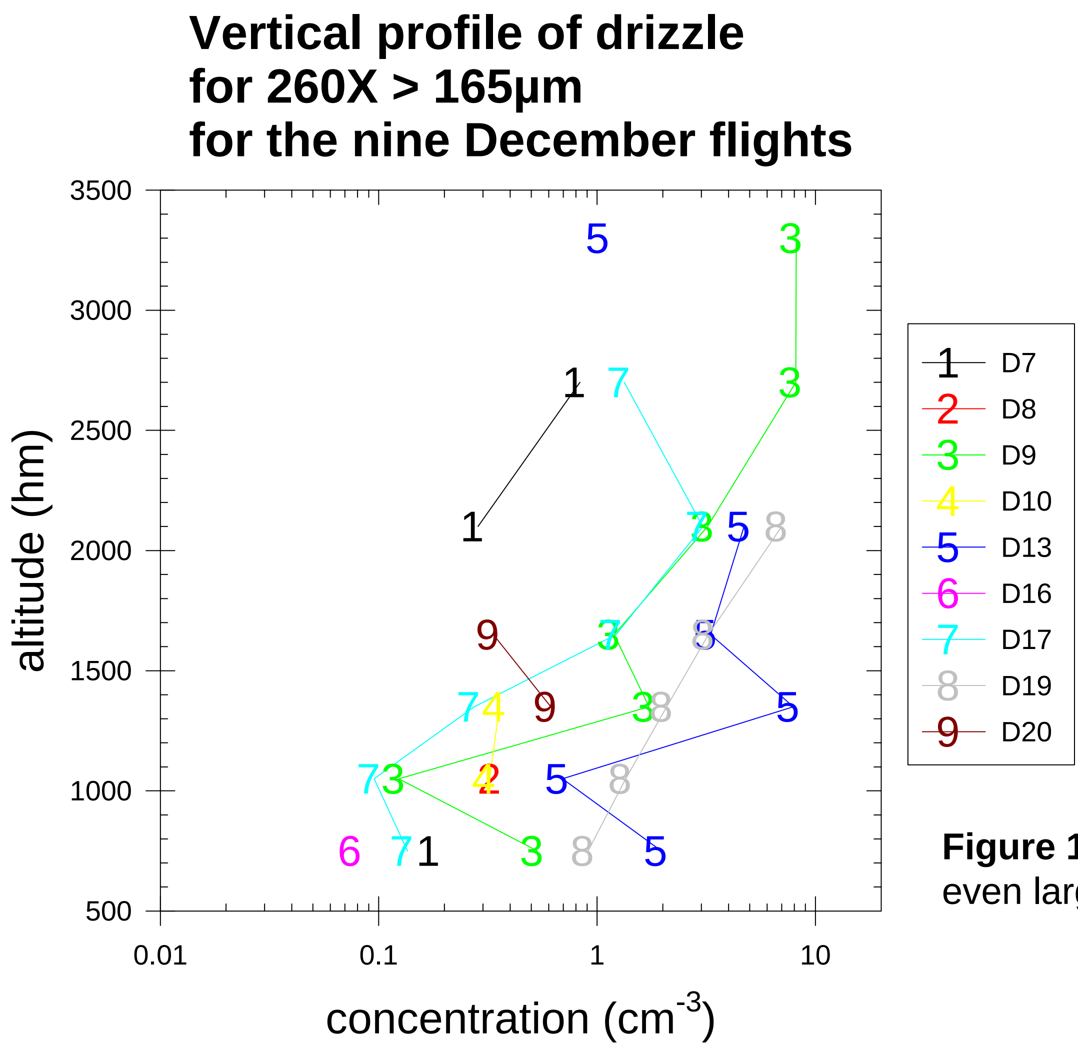

Figure 15. As Fig. 13 but for even larger drops (> 165 µm).

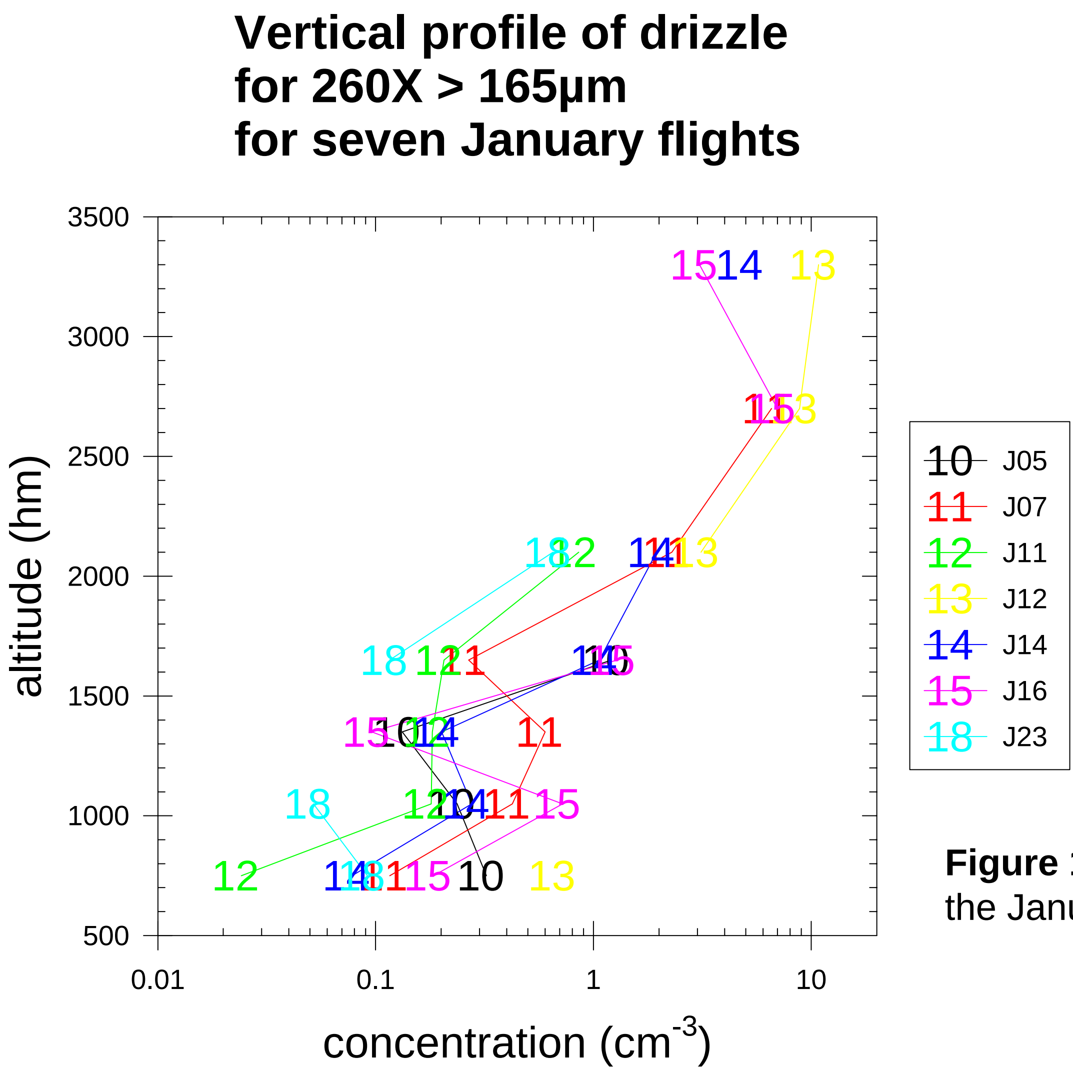

Figure 16. As Fig. 15 for the January flights.

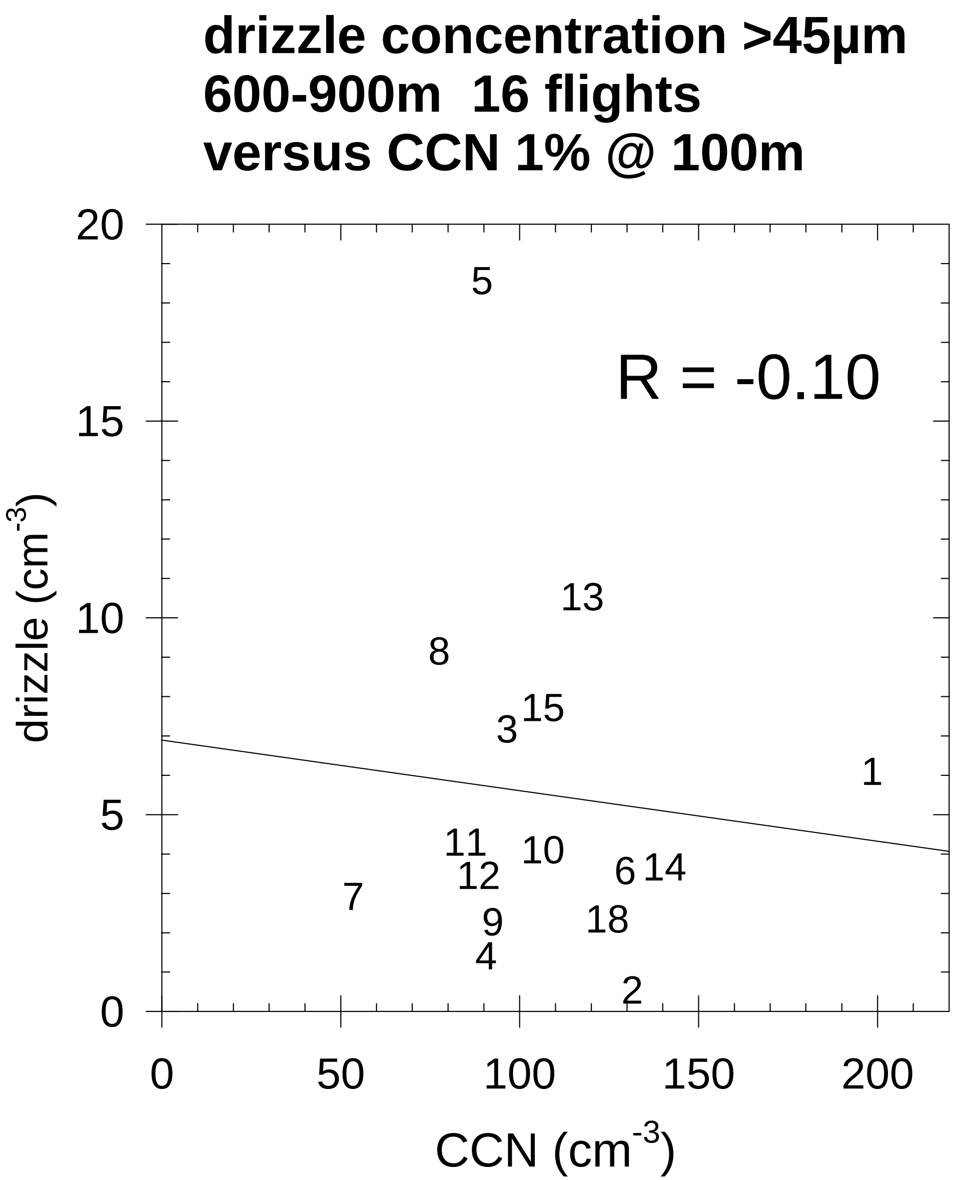

Figure 17. As Fig 1 but for drizzle drops > 45 µm measured by the 260X probe

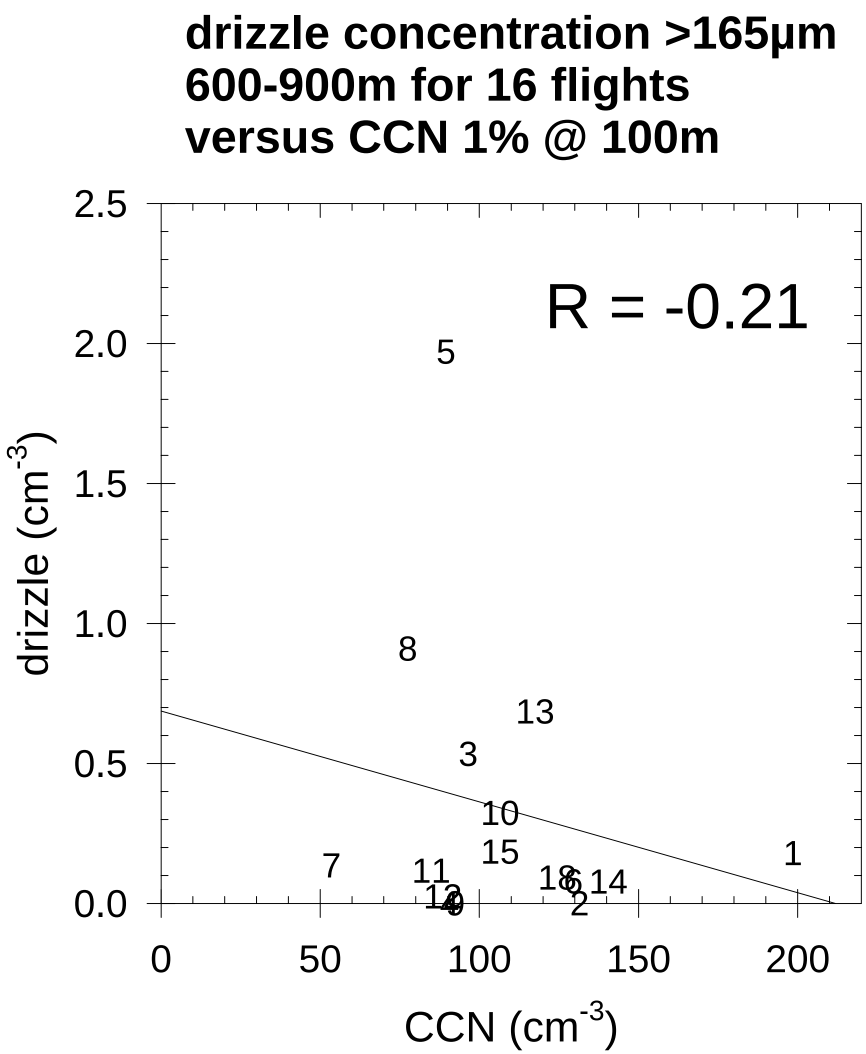

Figure 18. As Fig. 17 but for drops > 165 µm diameter.

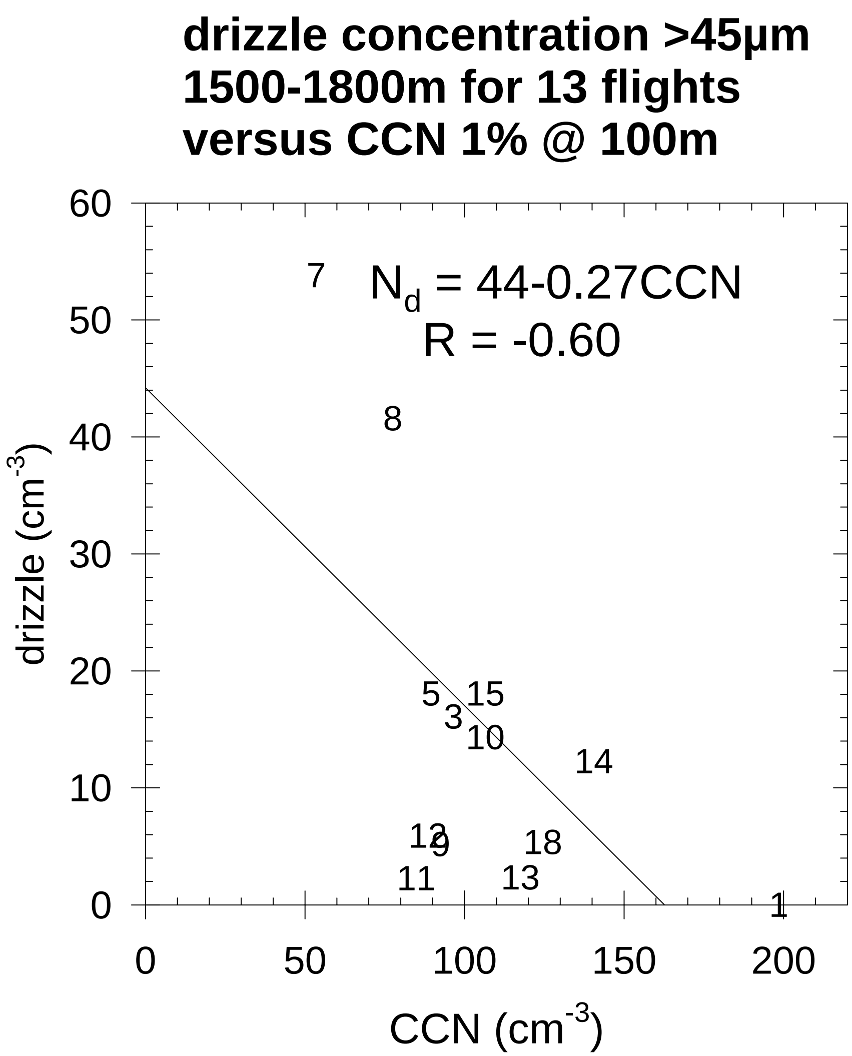

Figure 19. As Fig. 17 but for a higher altitude. Note the higher drop concentration range because of the greater amount of drizzle at higher altitudes (Figs. 13 and 14).

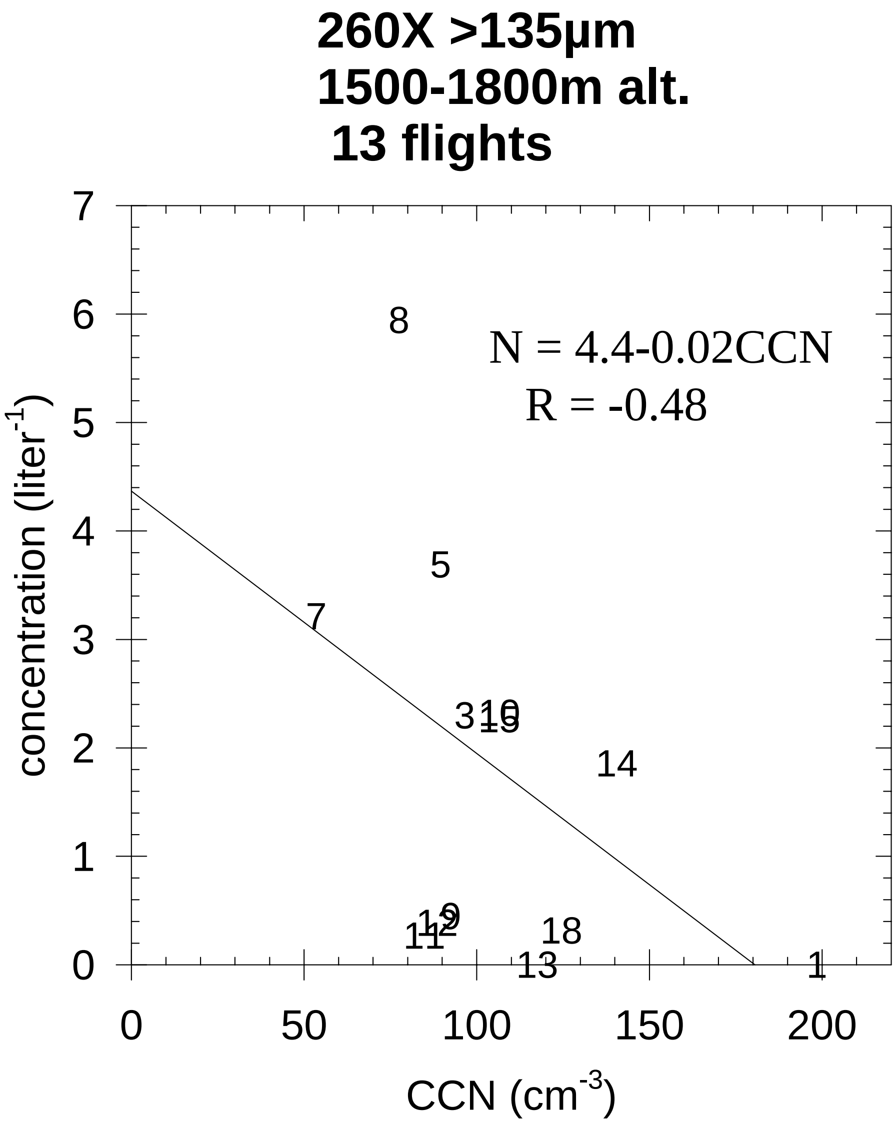

Figure 20. As Fig. 19 but for larger drizzle drops. Note the smaller scale due to the lower drop concentrations at the larger sizes.

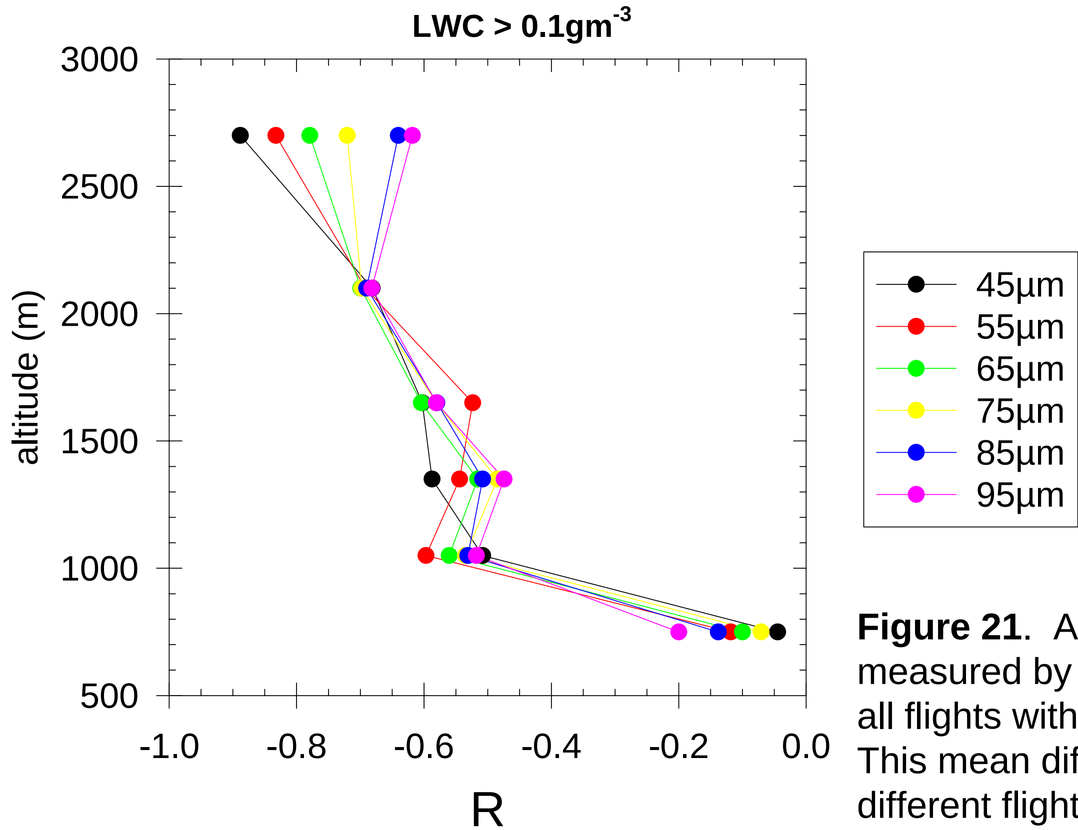

Figure 21. As Fig. 6 but for drizzle drops measured by the 260X probe. This includes all flights with data in each altitude band. This mean different numbers of flights and different flights at the various altitudes. 600-900m—16 flights (no RF17; same flights as the cloud data at this altitude noted in Fig. 6 caption); 900-1200m—15 flights (no RF13 or 17; same as cloud data noted in Fig. 6 caption); 1200-1500m—15 flights (no RF6 or 17; there was one more data point for the cloud data for this altitude as there was cloud data for RF17); 1500-1800m—13 flights (no RF2, 4, 6 or 17; this differs from the cloud data, which did have RF17 data but not RF11); 1800-2400m—12 flights (no RF2, 4, 6, 9, or 15; this is one more than the cloud data because there is drizzle data at this altitude for RF12); 2400-3000m—6 flights (no RF2, 4, 5, 6, 8, 9, 10, 12, 14, 17 or 18; the same flights as the cloud data at this altitude).

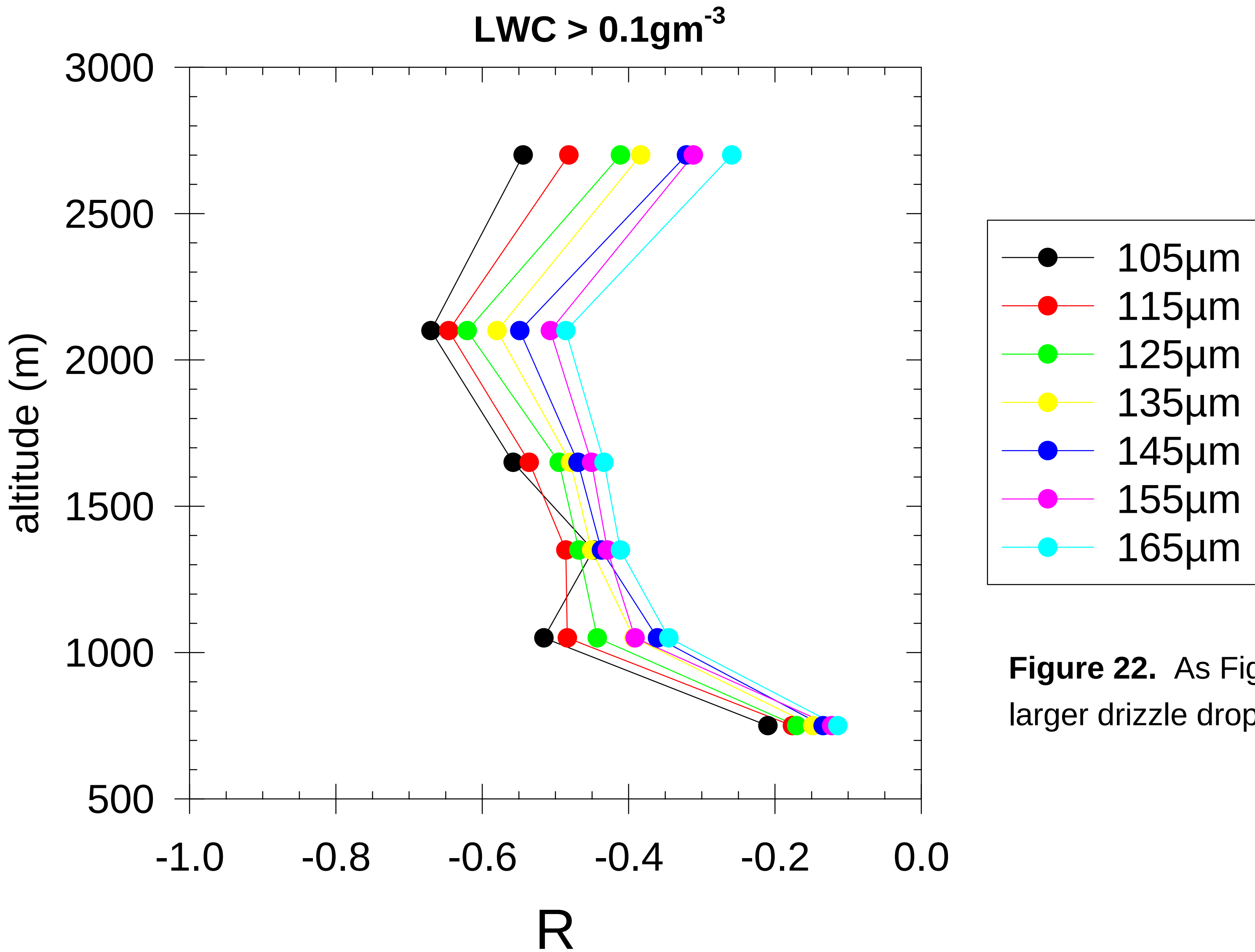

Figure 22. As Fig. 21 for larger drizzle drops.

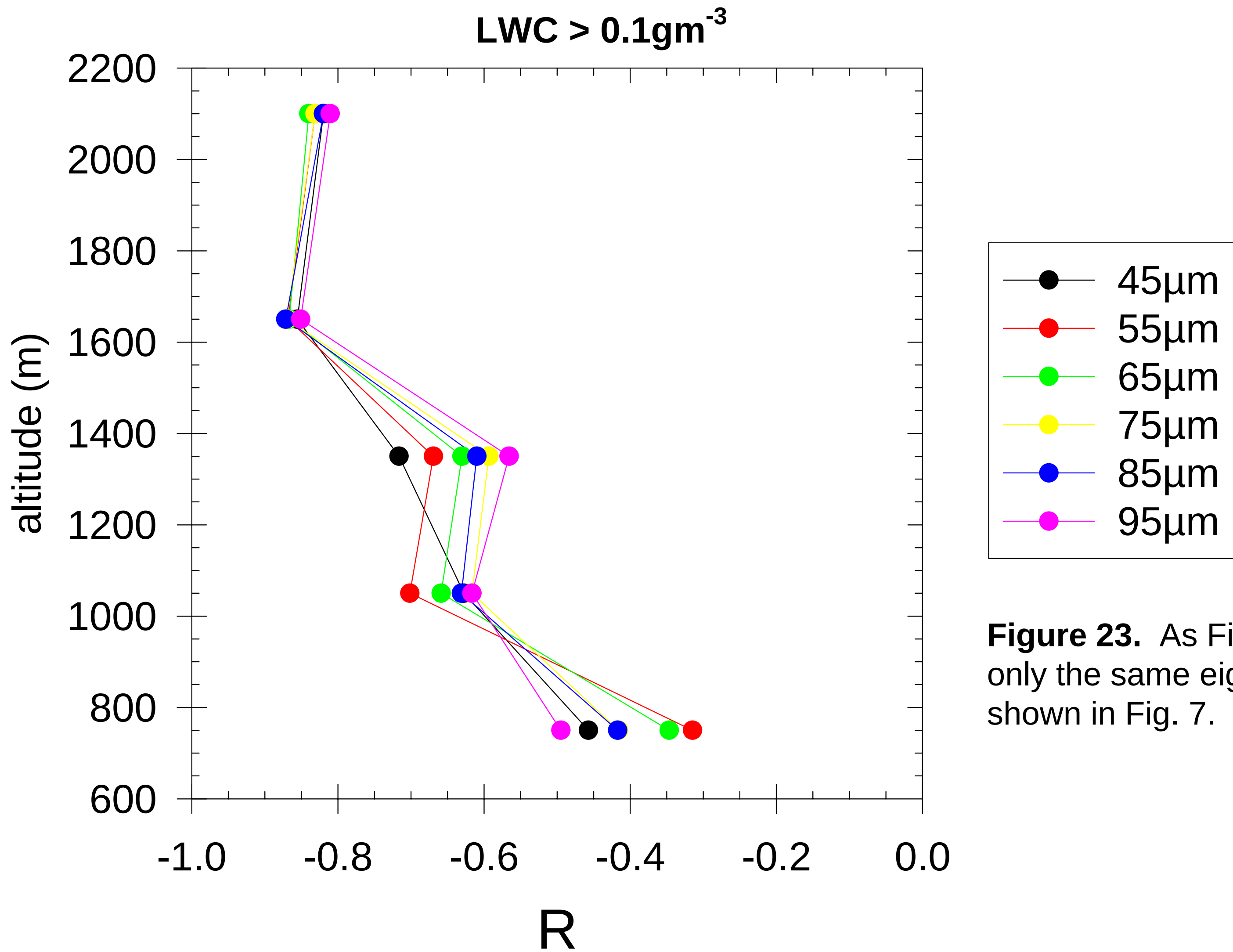

Figure 23. As Fig. 21 but for only the same eight flights shown in Fig. 7.

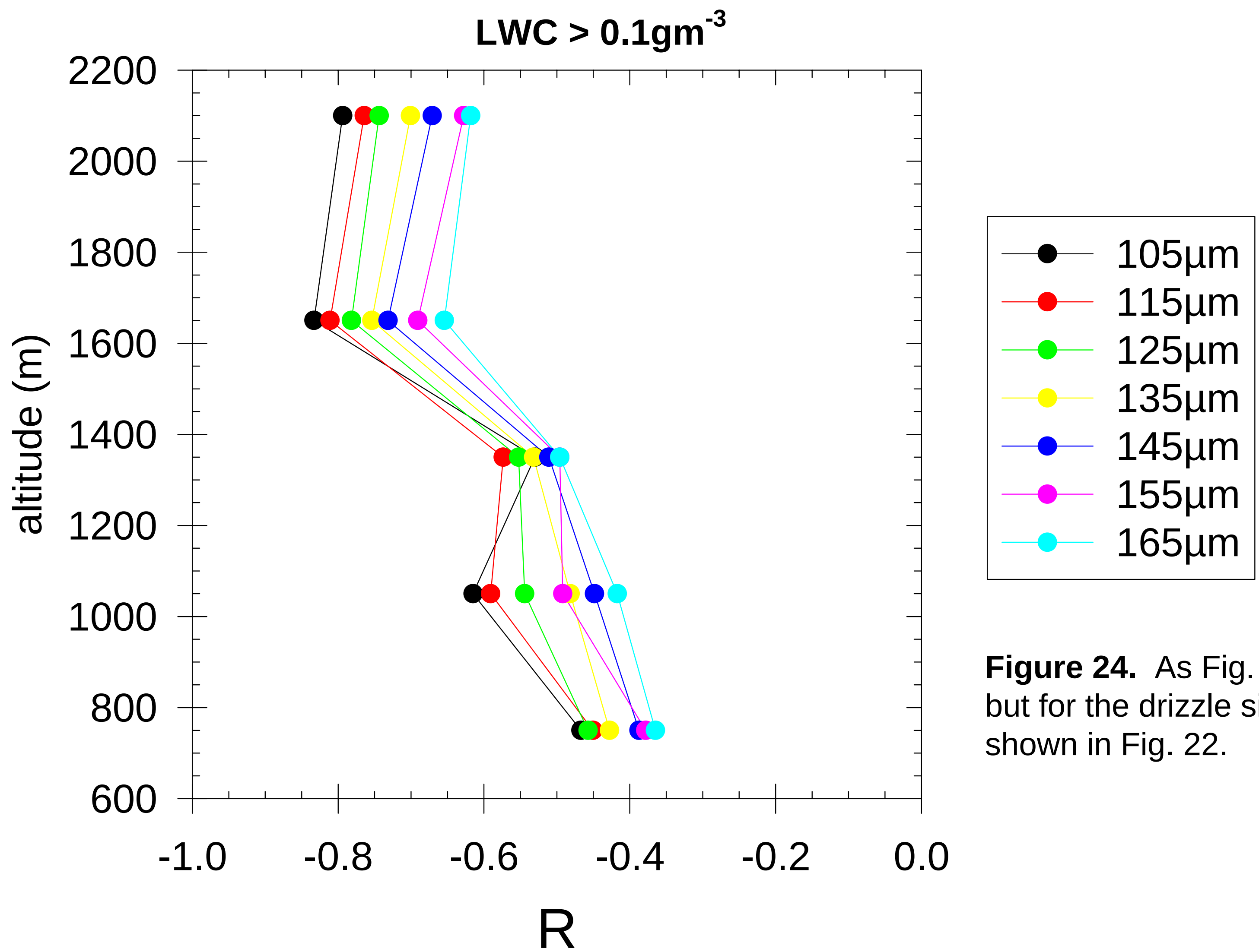

Figure 24. As Fig. 23 but for the drizzle sizes shown in Fig. 22.

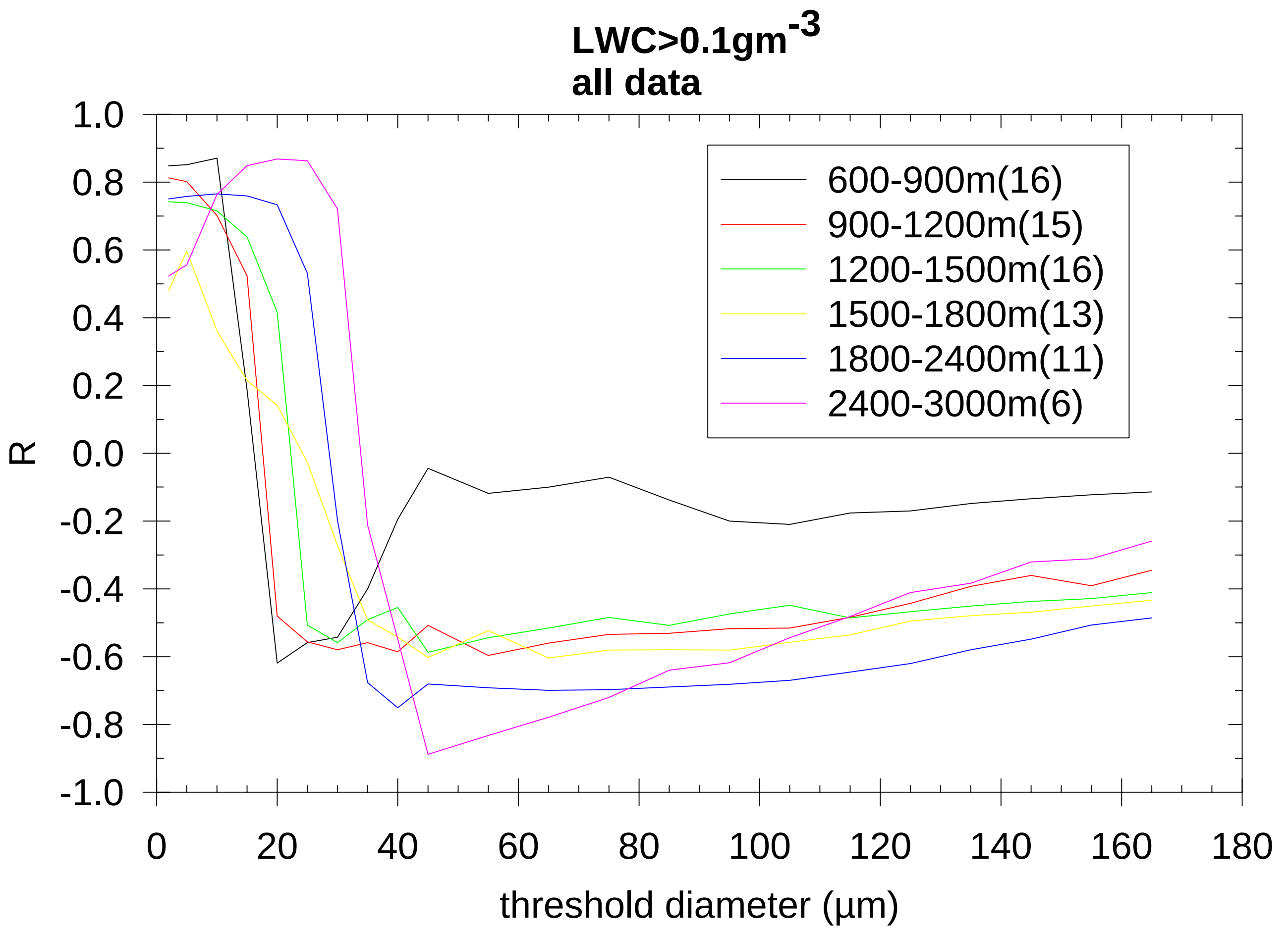

Figure 25. Correlation coefficients (R) displayed in Figs. 6, 21 and 22 displayed for each altitude band as a function of cumulative droplet size. As in those other figures the flights considered varied with altitude range and this may cause biases. The number of flights in each altitude range is shown in parentheses in the legend.

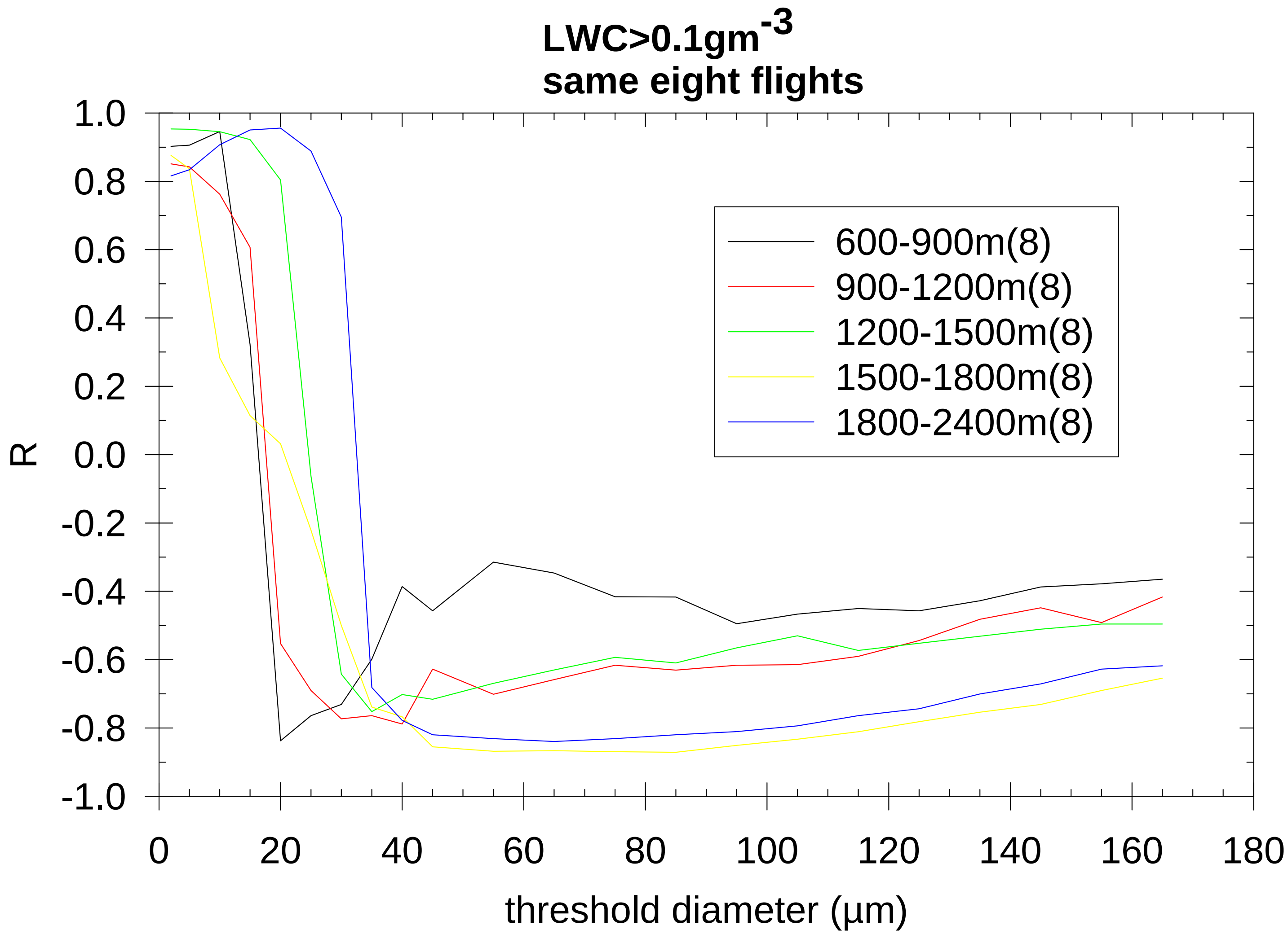

Figure 26. As Fig. 25 but for R displayed in Figs. 7, 23, and 24. The same eight flights are for all altitudes.

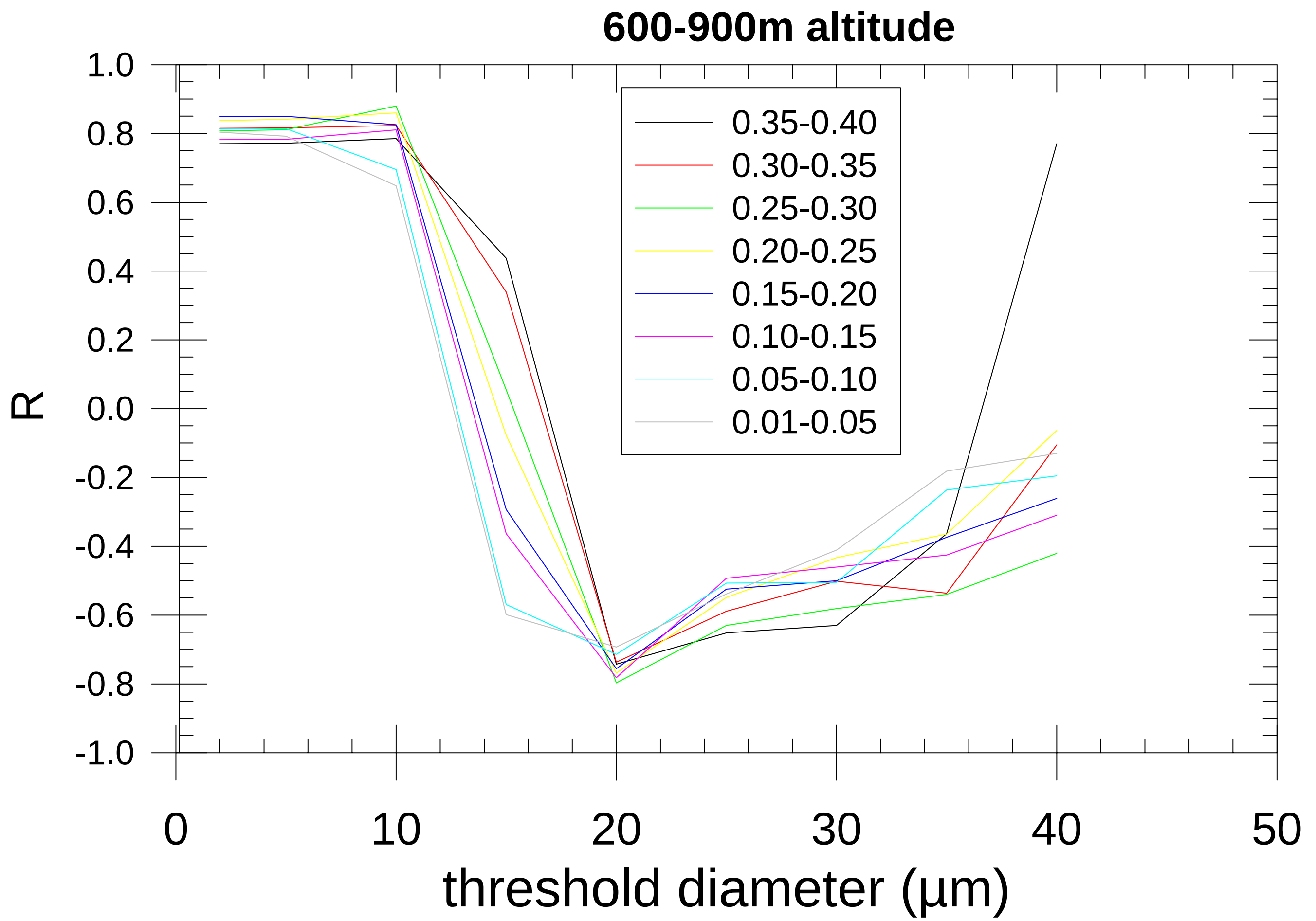

Figure 27. As Fig. 26 except that all data are from the 600-900m altitude range. The different lines are for various LWC ranges denoted in the legend. All data are from the same eleven flights that had data in these LWC intervals. This then excludes RF2, 4, 7, 11, 17 and 18 (D8, D10, D17, J7, J19, J23).

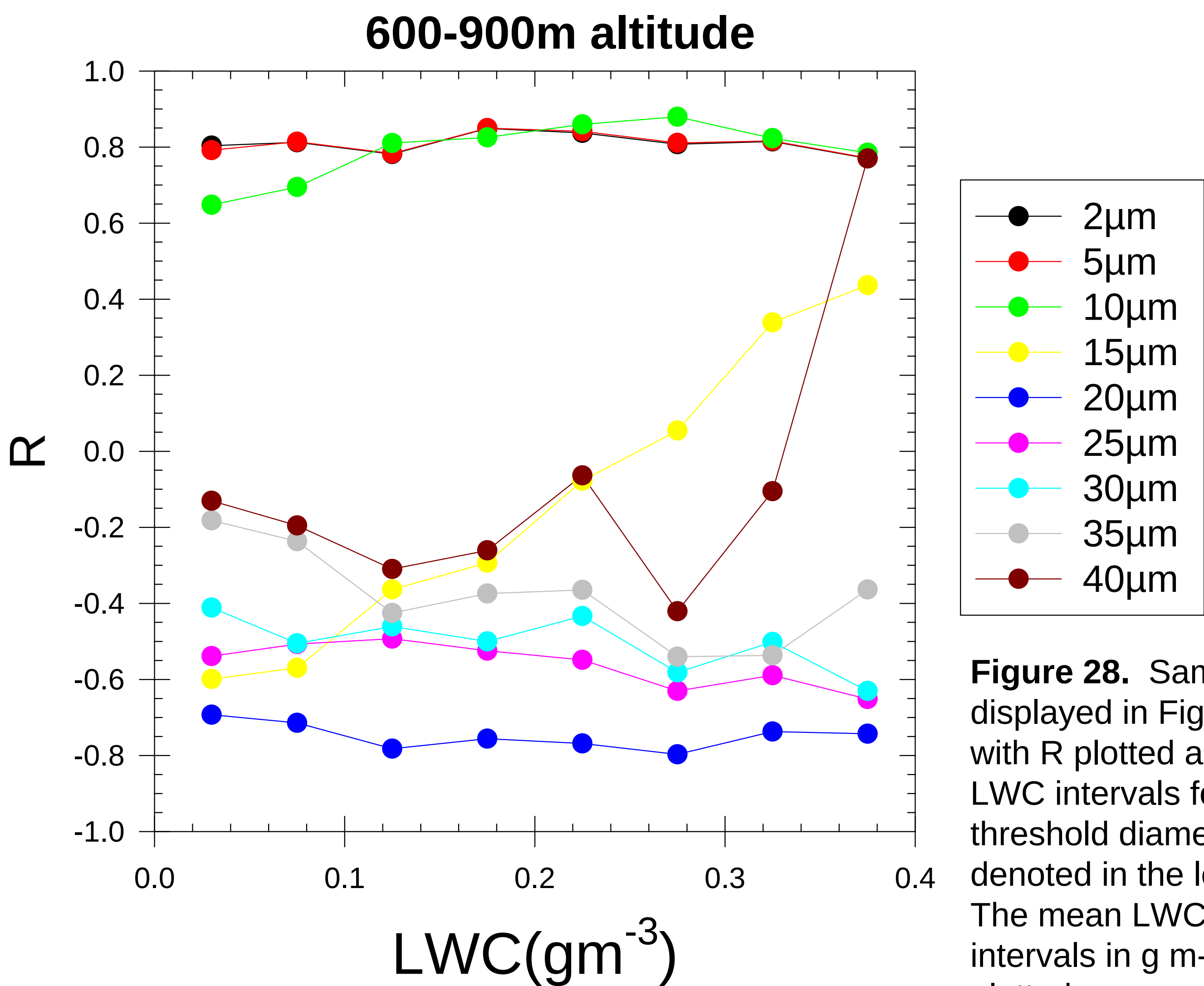

Figure 28. Same data displayed in Fig. 27, but with R plotted against LWC intervals for each threshold diameter denoted in the legend. The mean LWC of the intervals in g m-3 are plotted.

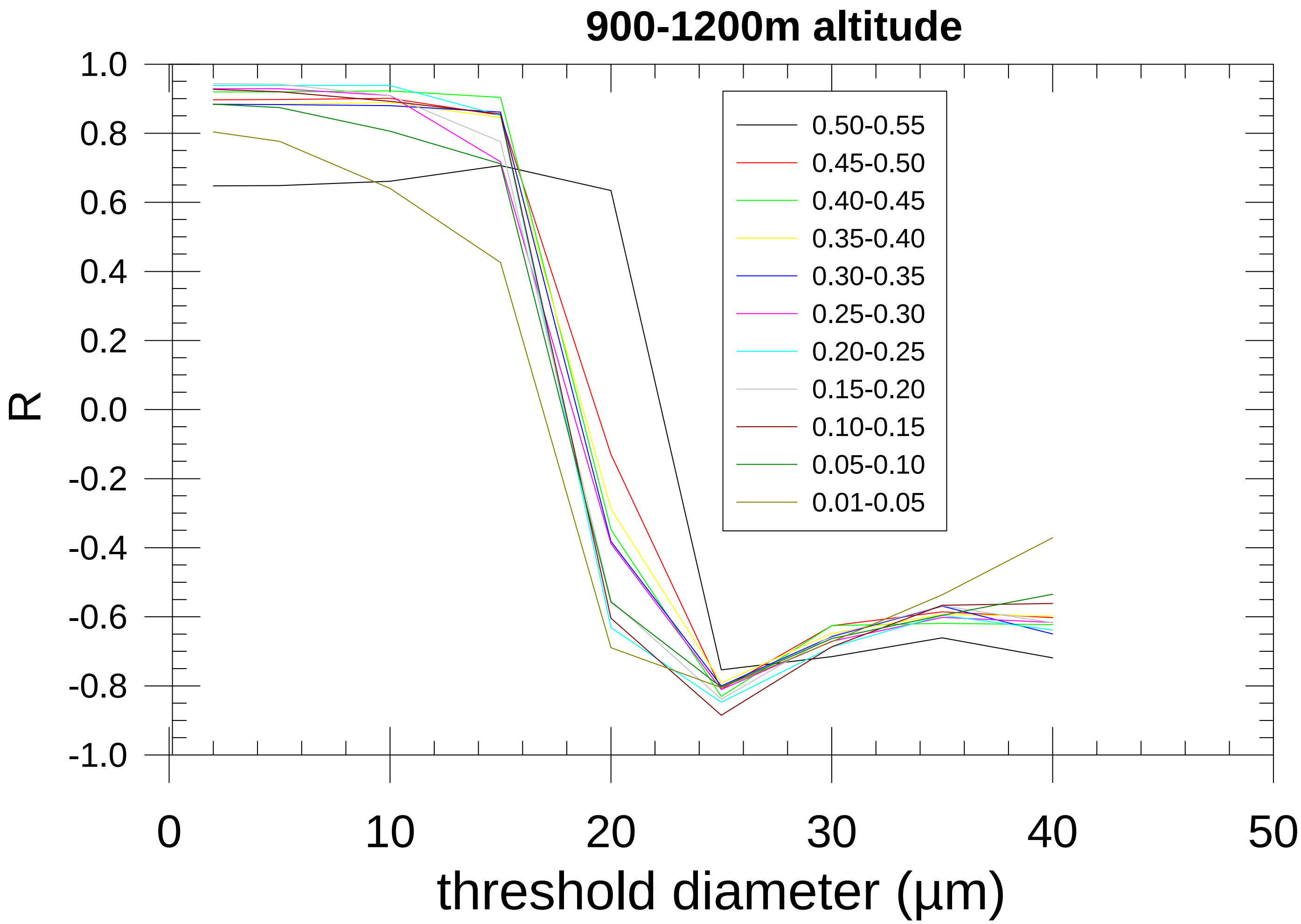

Figure 29. As Fig. 27, but for 900-1200m altitude range. There are also eleven flights with data in these LWC but they are different from the flights in Fig. 27. Here RF2, 3, 11, 13, 14 and 17 (D8, D9, J7, J12, J14 and J19) are excluded.

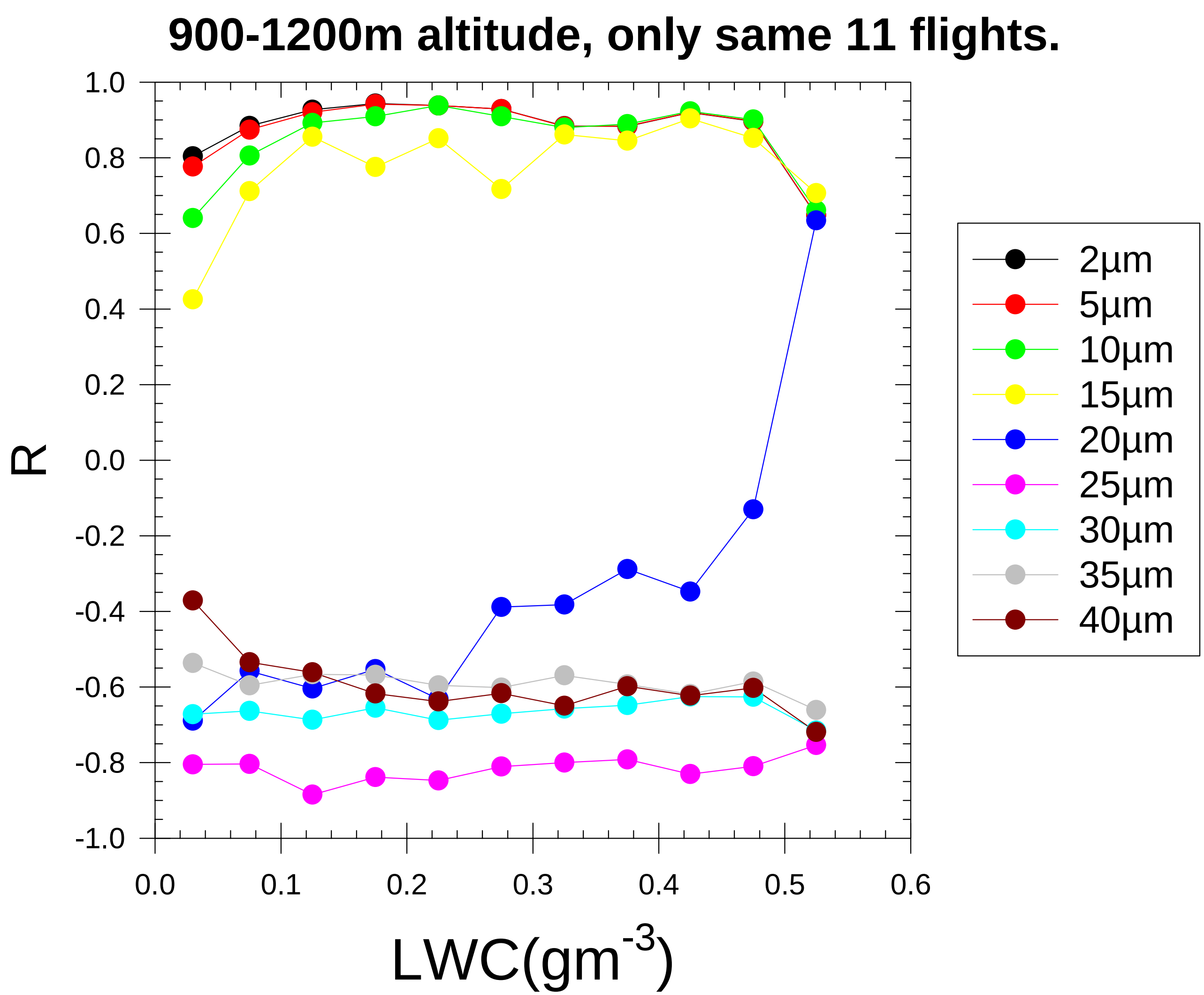

Figure 30. As Fig. 28 except that the data are from 900-1200m altitude range. The same data shown in Fig. 29.

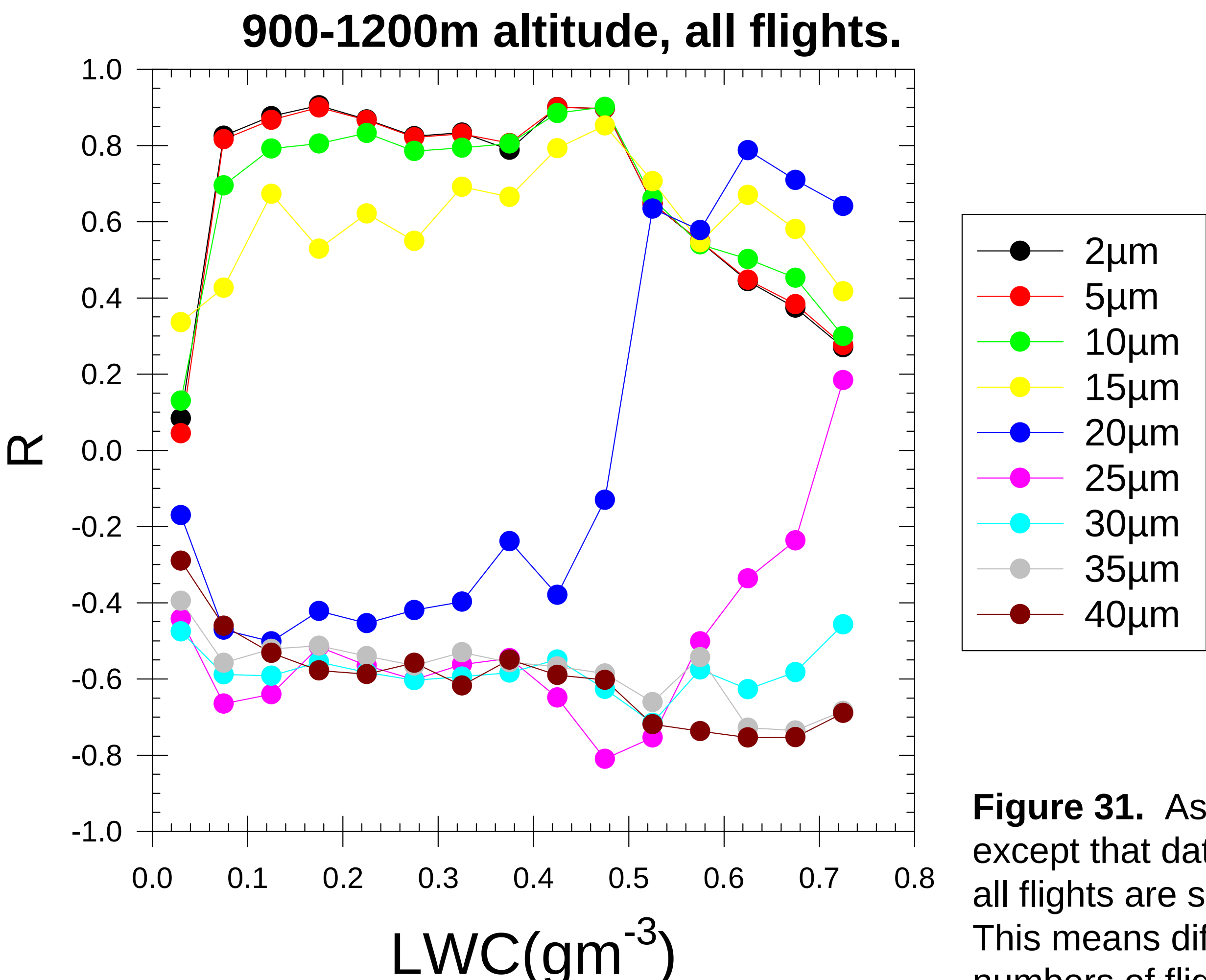

Figure 31. As Fig. 30 except that data from all flights are shown. This means different numbers of flights in the different LWC bands; six flights for 0.70-0.75, seven flights for 0.65-0.70, eight flights for 0.55-0.65, eleven flights for 0.45-0.55, twelve flights for 0.40-0.45, thirteen for 0.35-0.40, fifteen for 0.25-0.35, fourteen for 0.10-0.25 and sixteen for 0.01-0.10 g m-3.

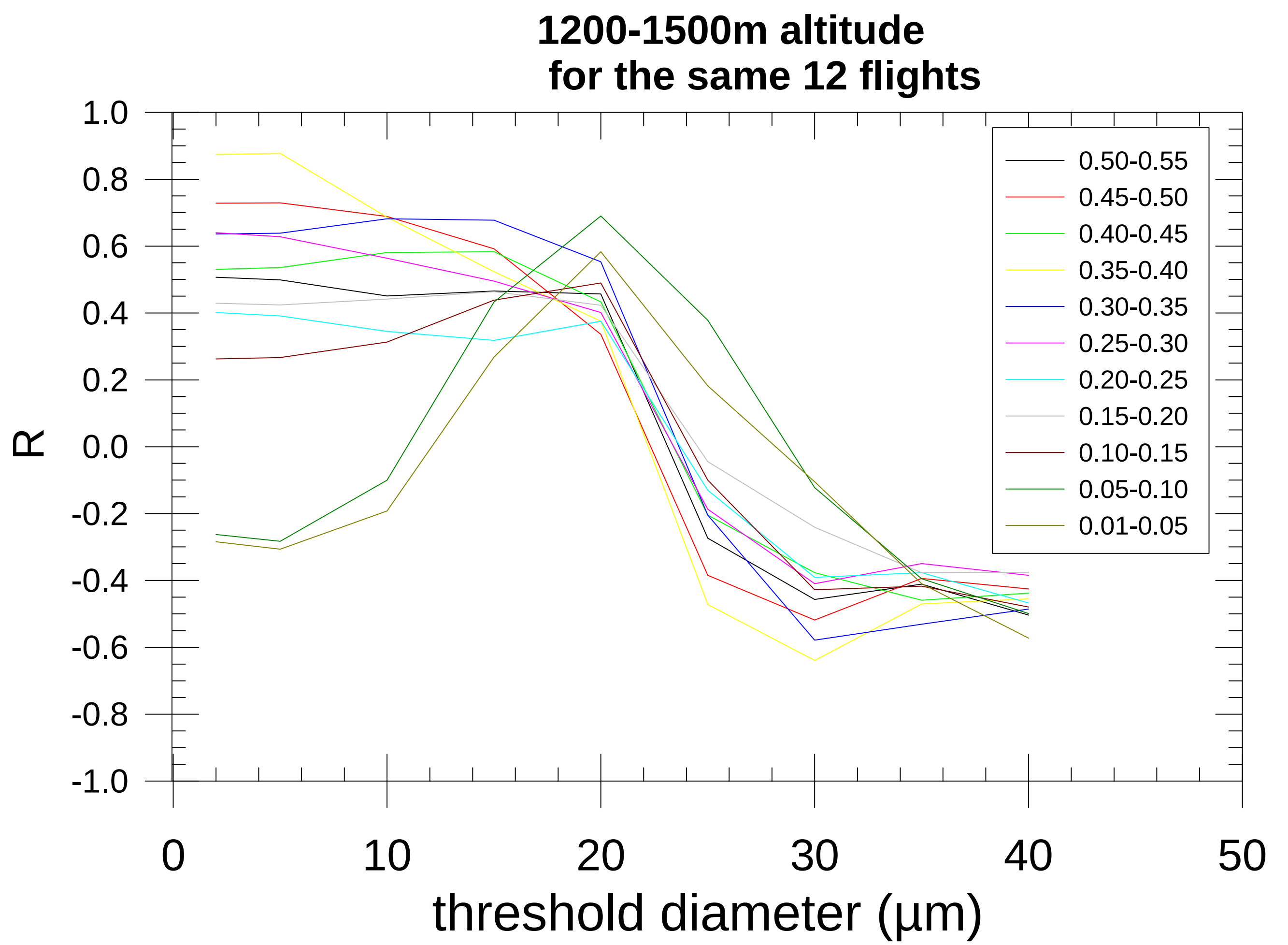

Figure 32. As Fig. 29, but for 1200-1500m altitude range. There are twelve flights with data in all of these LWC bins. Here RF1, 2, 6, 13 and 15 (D7, D8, D16, J12 and J16) are excluded.

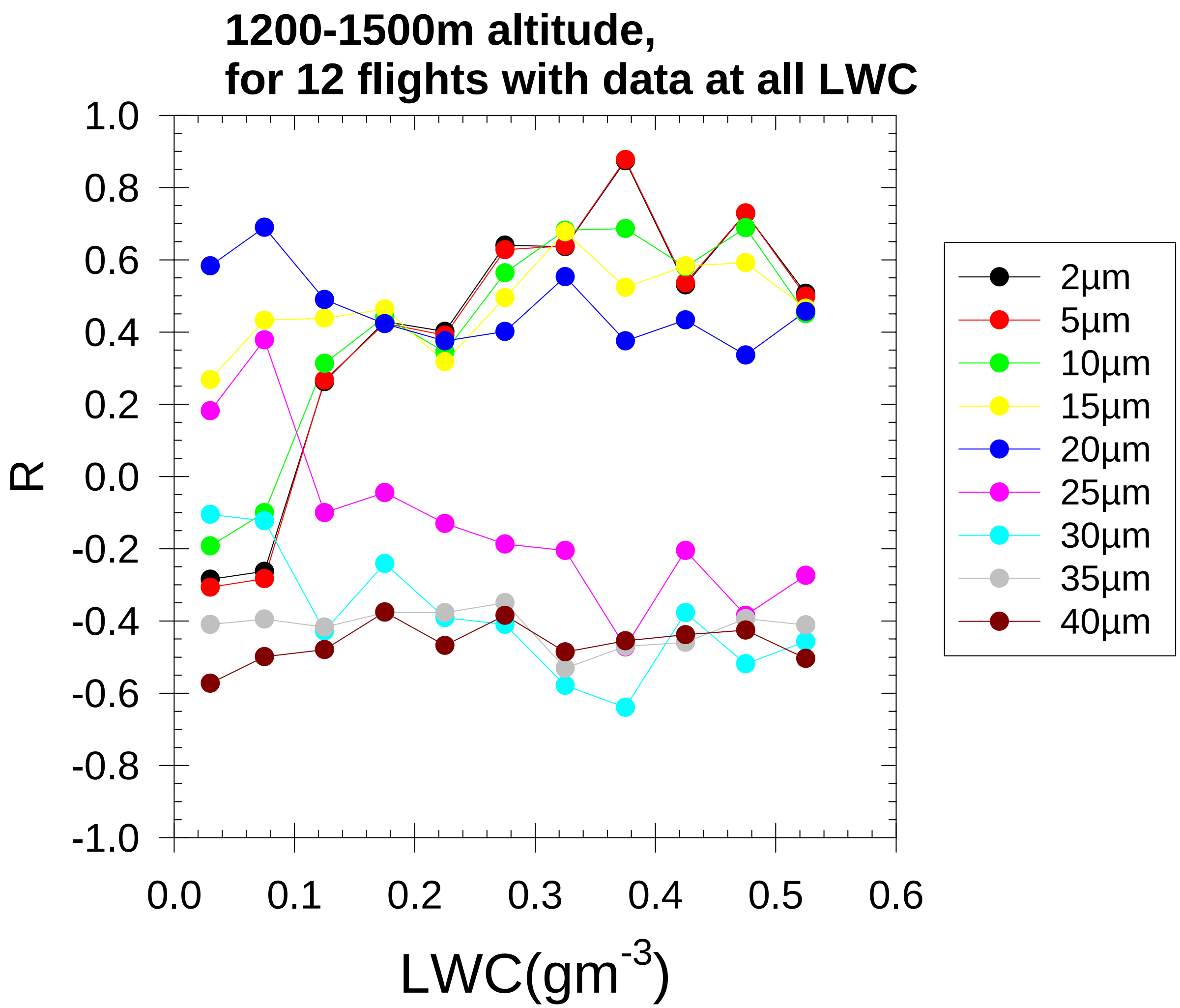

Figure 33. As Fig. 30 except that data are from 1200-1500m altitude range. The same data shown in Fig. 32.

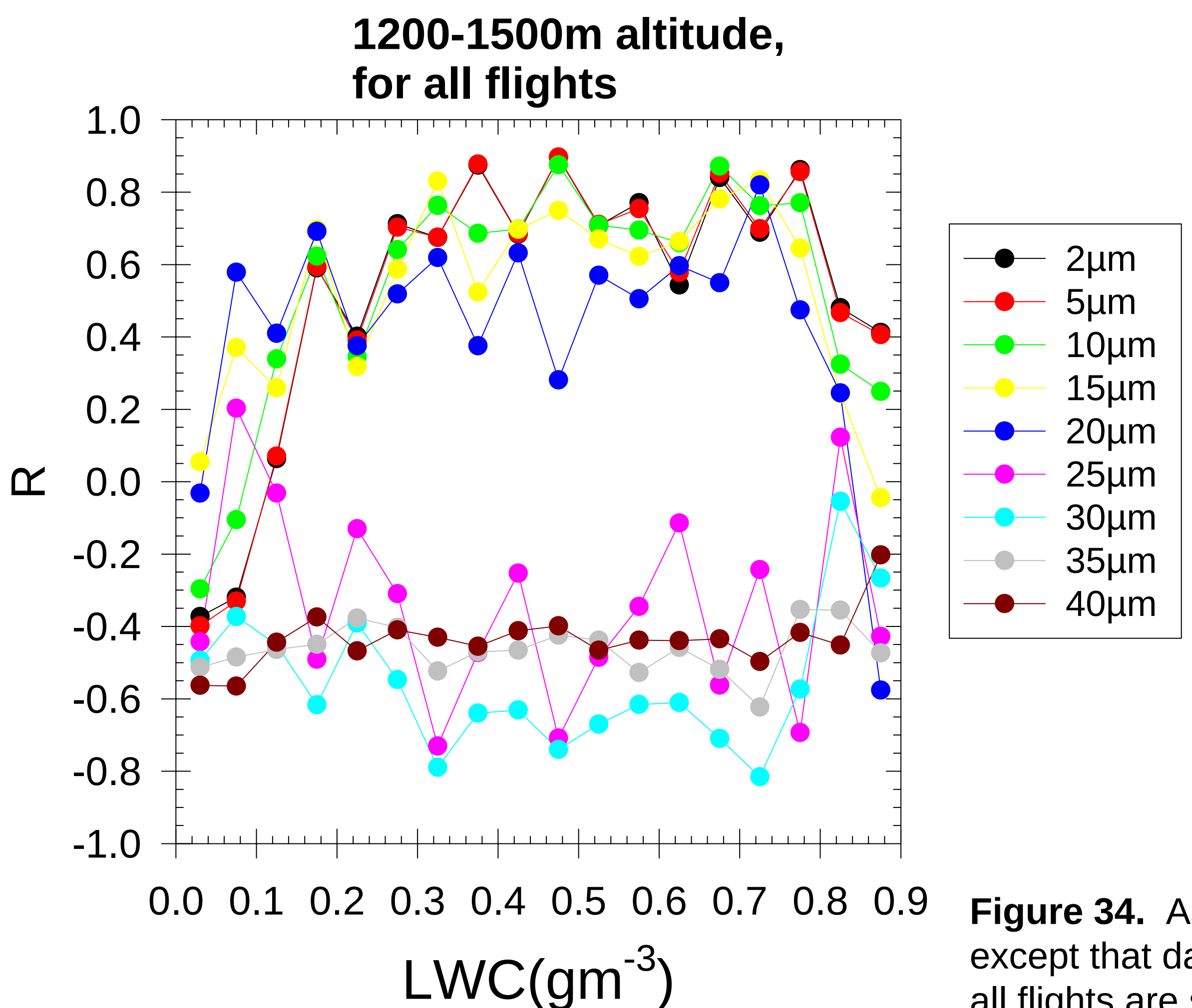

Figure 34. As Fig. 30 except that data from all flights are shown.

Five flights for 0.85-0.90, seven flights for 0.80-0.85, nine for 0.75-0.80, eleven for 0.60-0.75, thirteen for 0.55-0.60, 0.40-0.50 and 0.25-0.35, fourteen for 0.50-0.55 and 0.15-0.20, twelve for 0.35-0.40 and 0.20-0.25, fifteen for 0.05-0.15, and sixteen for 0.01-0.05 g m-3 LWC.

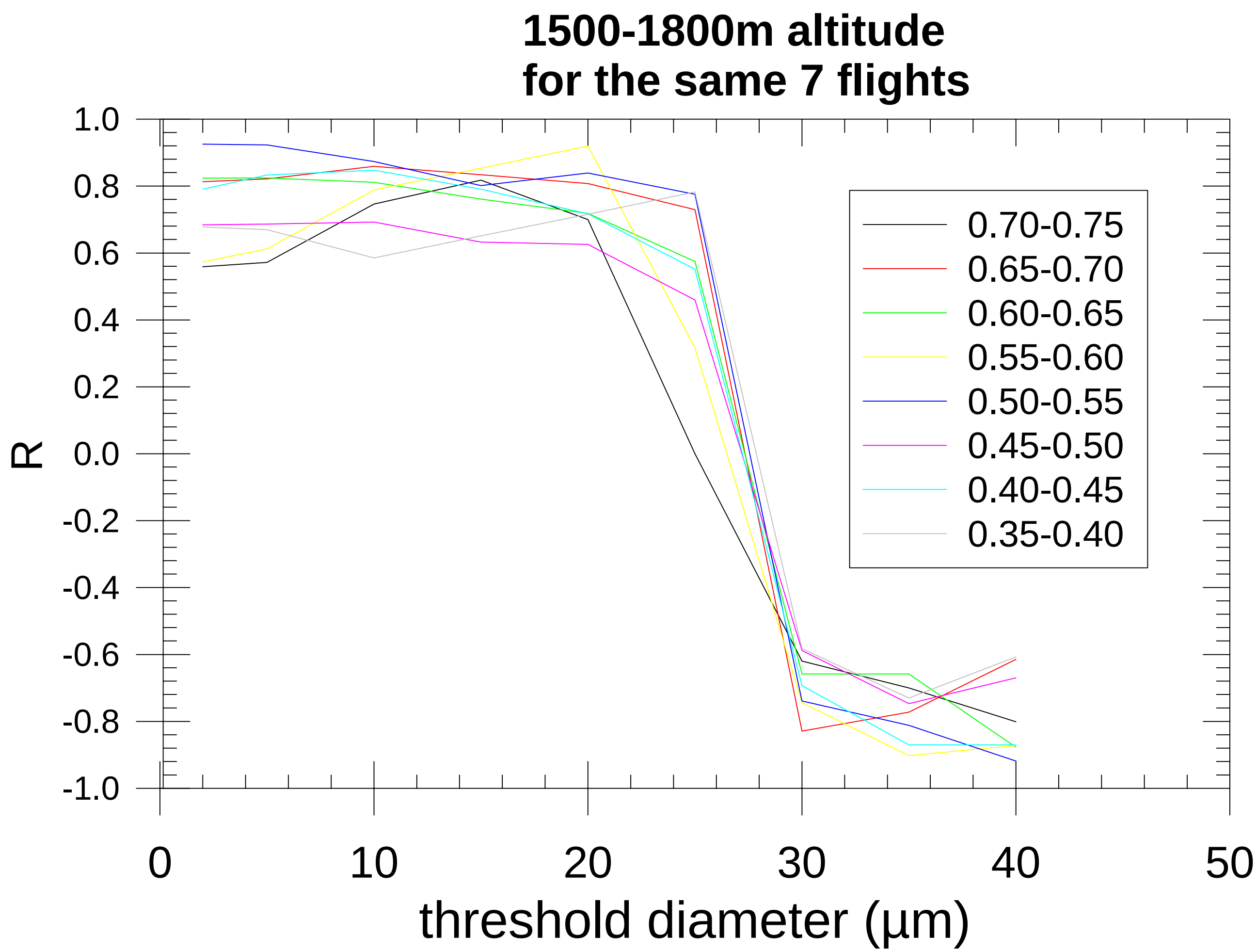

Figure 35. As Fig. 32, but for 1500-1800m altitude range. Here there are only 7 flights with data in all of the LWC bins shown. Here there is no data for RF1, 2, 3, 4, 6, 9, 11, 12, 13 and 17 (D7, D8, D9, D10, D16, D20, J7, J11, J12, J19).

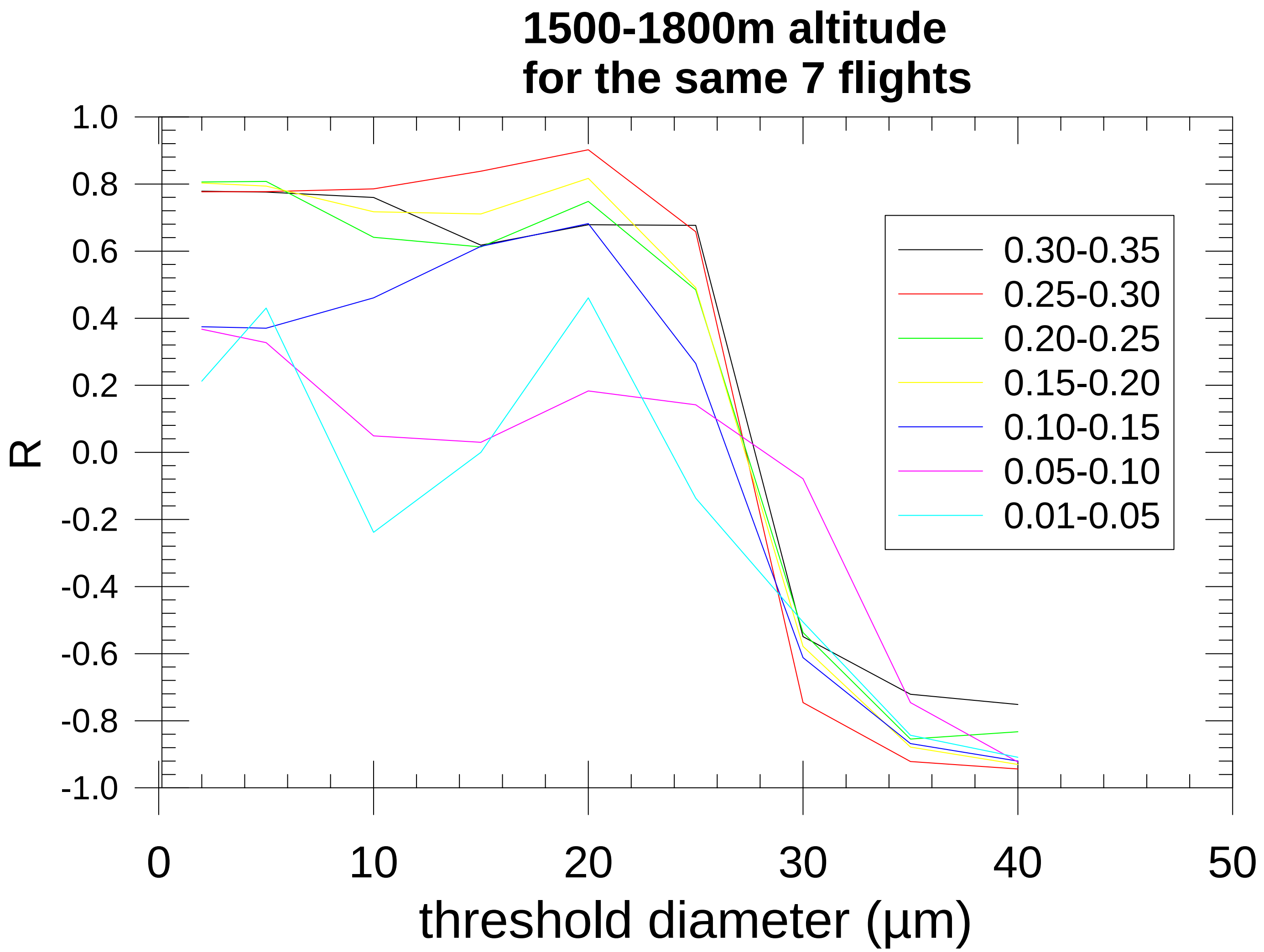

Figure 36. As Fig 35 for lower LWC bins. With so many more bins at this altitude it is necessary to use two figures.

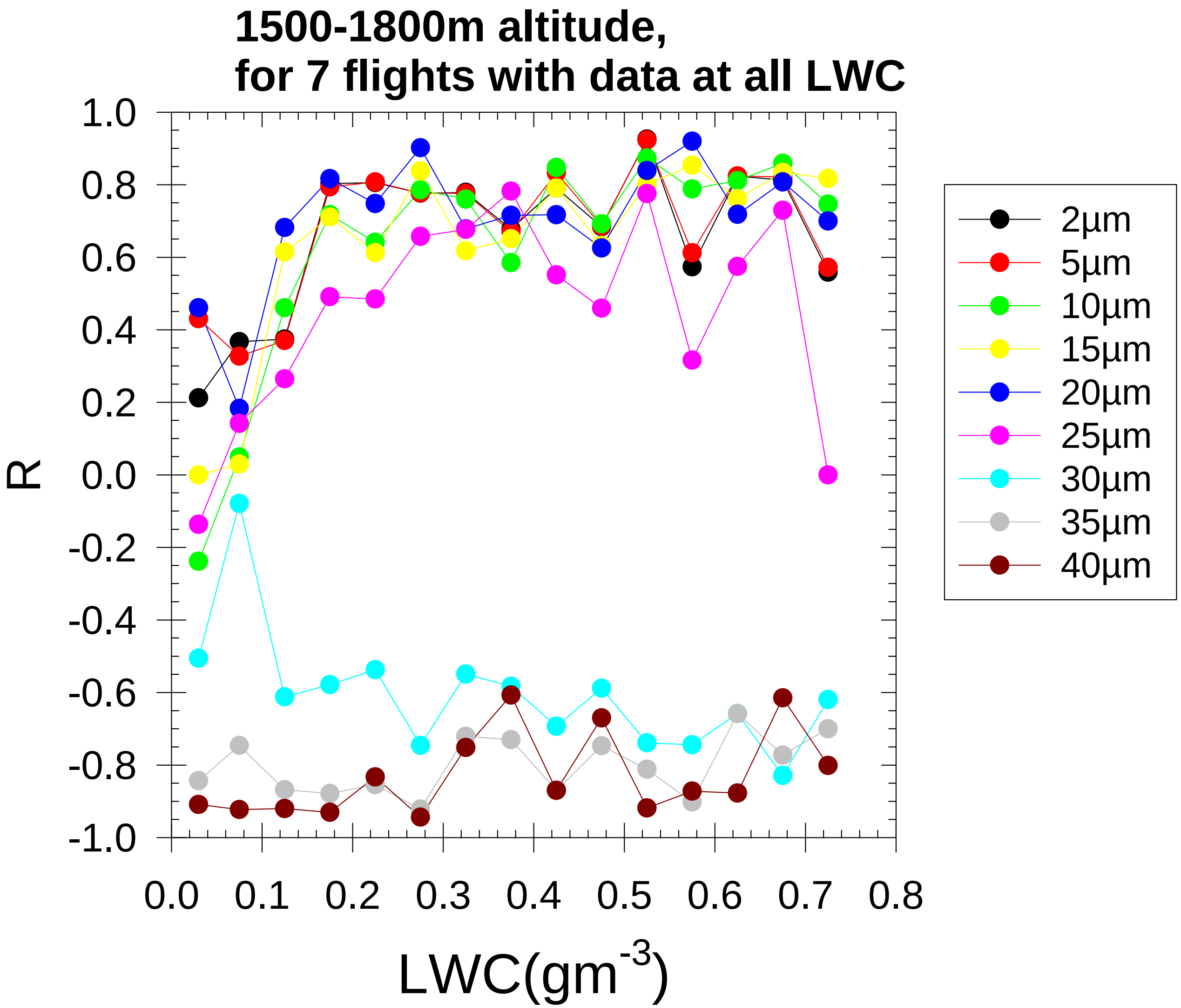

Figure 37. As Fig. 33 except that data are from 1500-1800m altitude range. The same data as shown in Figs. 35 and 36.